

Twitchin kinase interacts with MAPKAP kinase 2 in *Caenorhabditis elegans* striated muscle

Yohei Matsunaga, Hiroshi Qadota, Miho Furukawa, Heejoo (Helen) Choe, and Guy M. Benian
Department of Pathology, Emory University, Atlanta, GA 30322

ABSTRACT In *Caenorhabditis elegans*, twitchin is a giant polypeptide located in muscle A-bands. The protein kinase of twitchin is autoinhibited by 45 residues upstream (NL) and 60 residues downstream (CRD) of the kinase catalytic core. Molecular dynamics simulation on a twitchin fragment revealed that the NL is released by pulling force. However, it is unclear how the CRD is removed. To identify proteins that may remove the CRD, we performed a yeast two-hybrid screen using twitchin kinase as bait. One interactor is MAK-1, *C. elegans* orthologue of MAPKAP kinase 2. MAPKAP kinase 2 is phosphorylated and activated by p38 MAP kinase. We demonstrate that the CRD of twitchin is important for binding to MAK-1. *mak-1* is expressed in nematode body wall muscle, and antibodies to MAK-1 localize between and around Z-disk analogues and to the edge of A-bands. Whereas *unc-22* mutants are completely resistant, *mak-1* mutants are partially resistant to nicotine. MAK-1 can phosphorylate twitchin NL-Kin-CRD *in vitro*. Genetic data suggest the involvement of two other *mak-1* paralogues and two orthologues of p38 MAP kinase. These results suggest that MAK-1 is an activator of twitchin kinase and that the p38 MAP kinase pathway may be involved in the regulation of twitchin.

Monitoring Editor
Laurent Blanchoin
CEA Grenoble

Received: May 27, 2014
Revised: Apr 1, 2015
Accepted: Apr 1, 2015

INTRODUCTION

Muscle sarcomeres contain giant polypeptides (>700,000 Da) of the titin-like family, consisting primarily of multiple copies of immunoglobulin (Ig) and fibronectin type 3 (Fn3) domains and one or two protein kinase domains at their C-termini. These giant proteins are involved in sarcomere assembly and in sensing and transducing mechanical signals in the sarcomere (Kontrogianni-Konstantopoulos *et al.*, 2009; Krüger and Linke, 2011). These mechanical signals drive the development and regulation of muscle in adaptation to physical demands. Members of this family include titin and obscurin in mammals; UNC-22 (twitchin), UNC-89 (obscurin), and TTN-1 in *Caenorhabditis elegans*; twitchin in molluscs; and projectin (quite similar to twitchin), UNC-89, and stretchin in insects (Bullard *et al.*, 2002; Kontrogianni-Konstantopoulos *et al.*, 2009).

Bacterially expressed *C. elegans* twitchin kinase has protein kinase activity *in vitro*, both in autophosphorylation and toward peptides derived from vertebrate myosin light chains (Lei *et al.*, 1994; Heierhorst *et al.*, 1996). Twitchin kinase is autoinhibited by a 60-residue-long regulatory tail that lies just C-terminal of the kinase catalytic core (called the C-terminal regulatory domain [CRD]; Lei *et al.*, 1994). Crystal structures of twitchin kinase from *C. elegans* (Hu *et al.*, 1994) and *Aplysia* (Kobe *et al.*, 1996) and from human titin kinase (Mayans *et al.*, 1998) show that the CRD wedges itself between the two subdomains of the catalytic core, blocking binding sites for ATP and protein substrates. Activation of these kinases requires removal of the CRD from the active site, but how this occurs is unknown. Steered molecular dynamics simulations on human titin kinase indicate that small pulling forces occurring during muscle activity are sufficient to remove the CRD from the catalytic pocket and permit access to substrates and, thus, catalytic activity (Grater *et al.*, 2005). Although this model has not been proven by experiments, atomic force microscopy (AFM) experiments on titin kinase demonstrate that pulling force permits ATP to bind to the kinase (Puchner *et al.*, 2008; Puchner and Gaub, 2010). In addition, there is some evidence that stretching force activates twitchin kinase in *Mytilus*: using permeabilized smooth muscles, Butler and Siegelman (2011) demonstrated that with a 10% stretch there is a twofold increase in phosphorylation of a model peptide substrate that previously had been

This article was published online ahead of print in MBoC in Press (<http://www.molbiolcell.org/cgi/doi/10.1091/mbc.E14-05-1009>) on April 7, 2015.

Address correspondence to: Guy Benian (pathgb@emory.edu).

Abbreviations used: CRD, C-terminal regulatory domain; GFP, green fluorescent protein; GST, glutathione *S*-transferase; MBP, maltose-binding protein; NL, N-terminal linker; Y2H, yeast two-hybrid.

© 2015 Matsunaga *et al.* This article is distributed by The American Society for Cell Biology under license from the author(s). Two months after publication it is available to the public under an Attribution–Noncommercial–Share Alike 3.0 Unported Creative Commons License (<http://creativecommons.org/licenses/by-nc-sa/3.0>). "ASCB," "The American Society for Cell Biology," and "Molecular Biology of the Cell" are registered trademarks of The American Society for Cell Biology.

shown to be a substrate for molluscan twitchin kinase in vitro. Moreover, the titin kinase CRD binds as a complex to the autophagosome receptors nbr1 and p62 and the E3 ubiquitin ligase MuRF2 (Lange *et al.*, 2005). Force-dependent regulation of this complex was suggested by finding that in cultured cardiac muscle cells, when induced to stop beating, there was disassembly of this complex and nuclear translocation of MuRF2. Correlated nuclear export of serum response factor resulted in decreased transcription of mRNAs for sarcomeric proteins (Lange *et al.*, 2005). Force was initially believed to induce phosphorylation by titin kinase of nbr1 and/or p62, and this might explain decreased binding affinity, and, at least in vitro, nbr1 and p62 could be weakly phosphorylated by titin kinase (Lange *et al.*, 2005). However, more recently, titin kinase has been demonstrated to be an inactive pseudokinase (Bogomolovas *et al.*, 2014).

The crystal structure of the largest segment of any giant kinase, the Fn-N-terminal linker (NL)-kinase-CRD-Ig segment from *C. elegans* twitchin, has been reported (von Castelmur *et al.*, 2012). Molecular dynamic simulations indicate that, unexpectedly, the mechanically sensitive portion is an NL of 45 residues lying between the Fn3 domain and the kinase catalytic core, not the CRD. In fact, the CRD remains attached to the large lobe of the kinase even after the small lobe has been unwound. In mammalian titin kinases, the NL sequence is shorter, ~26 residues long (von Castelmur *et al.*, 2012), and was not present in the original crystal structure (Mayans *et al.*, 1998) or the molecular dynamics simulations (Grater *et al.*, 2005). However, in AFM pulling experiments on a larger segment of human titin including Ig-Ig-Fn-NL-Kin-CRD-Ig-Ig, the first unfolding peak was attributed to the unfolding of a "23-residue" NL (Puchner *et al.*, 2008). Therefore the NL of mammalian titin kinase may also be mechanically sensitive.

For nematode twitchin kinase, in vitro kinase assays using a model peptide substrate show that NL and CRD each inhibits kinase activity by one-half (von Castelmur *et al.*, 2012). One possibility is that the purpose of this CRD interaction is to stabilize the kinase catalytic core and protect its active site from being destroyed. Another possibility is that under some physiological conditions, twitchin kinase needs to be fully activated by pulling force removing the NL and additional, unknown factors removing the CRD from the catalytic pocket. These unknown factors could be binding to other protein activators or phosphorylation by another kinase. Twitchin kinase is 52% identical in sequence to chicken smooth muscle myosin light chain kinase (MLCK; Benian *et al.*, 1989). MLCKs are also autoinhibited by an ~60-residue tail C-terminal of their catalytic core (Kemp *et al.*, 1987) and are activated upon binding of this autoinhibitory sequence to calmodulin (Stull *et al.*, 1986). Although calmodulin binds to the CRD of twitchin kinase in vitro, it does not lead to significant activation (Lei *et al.*, 1994).

In *C. elegans*, *unc-22* is one of ~40 genes that, when mutant, result in slow or paralyzed adult nematodes and disorganized sarcomeric structure ("*unc*" for "uncoordinated"; Waterston *et al.*, 1980; Zengel and Epstein, 1980). The *unc-22* gene encodes twitchin, a ~754-kDa polypeptide consisting primarily of 31 Fn3 domains, 30 Ig domains, and a single protein kinase domain near its C-terminus (Moerman *et al.*, 1986, 1988; Benian *et al.*, 1989, 1993). The sequence of *C. elegans* twitchin revealed that it was the first intracellular protein to join the Ig superfamily and helped define the intracellular, mostly muscle, branch of this superfamily. *unc-22* mutants display a characteristic "twitching" of the animal's surface, ~1–2 times/s, which originates from the underlying muscle, and also show variably disorganized sarcomeres (Waterston *et al.*, 1980; Moerman *et al.*, 1988). Whether twitching represents unregulated contraction or relaxation is unknown, but twitching is enhanced by

choline agonists such as nicotine (Moerman and Baillie, 1979). Indeed, whereas exposure to nicotine causes wild-type nematodes to stop moving, *unc-22* mutants continue to move and twitch violently. Moreover, although under typical culture conditions, *unc-22* heterozygotes move normally and have normal muscle structure, in nicotine solutions, they twitch; that is, *unc-22* is "conditionally dominant" (Moerman and Baillie, 1979). Because this dominance occurs even with null alleles, this suggests that twitchin is required stoichiometrically. Genetic data strongly suggest interaction of twitchin with myosin: an *unc-22*-null allele shows disorganization of thick filaments (Moerman *et al.*, 1988), and rare missense alleles of *unc-54* residing in the head domain of myosin heavy chain B suppress the twitching of *unc-22* mutants and also improve their locomotion and muscle structure (Moerman *et al.*, 1982).

To determine what might remove the CRD and permit full activation, we used a region of *C. elegans* twitchin containing the kinase catalytic core and the CRD to screen a yeast two-hybrid library. Our bait included the N-terminal 45 residues of the 60-residue CRD, based on results of titin kinase yeast two-hybrid screening: titin kinase including a truncated but not full-length CRD was found to interact with Nbr1 (Lange *et al.*, 2005). We found that twitchin kinase interacts with MAK-1, an orthologue of mammalian mitogen-activated protein (MAP) kinase-activated protein (MAPKAP) kinase 2, known to be phosphorylated and thereby activated by p38 MAP kinase.

RESULTS

Identification of MAK-1 as a binding partner for twitchin kinase

To identify proteins that might regulate the activity of the protein kinase domain of twitchin, we used Ig25-Fn31-NL-Kin-CRD (45 amino acids [aa]) as bait to screen a yeast two-hybrid (Y2H) library of *C. elegans* cDNAs (Figure 1A). A total of 1.7×10^6 colonies were screened, and we obtained 82 prey clones that were positive upon retransformation, identifying 26 genes (Supplemental Table S1). We then queried Serial Analysis of Gene Expression (SAGE) data available in Meissner *et al.* (2009) to identify which of these genes were primarily expressed in body wall muscle. Many of the genes are expressed in multiple tissues (muscle, neurons, and gut), and several others are expressed primarily in neurons. Two genes are primarily expressed in muscle, *deb-1* and K08F8.1. *deb-1* encodes vinculin, a component of the base of the dense body (Z-disk analogue; Barstead and Waterston, 1989), but this interaction does not seem biologically relevant, as twitchin is located in a different portion of the sarcomere, the A-band (Moerman *et al.*, 1988). K08F8.1, which we renamed *mak-1* (see later discussion), caught our attention because the encoded protein is an orthologue of a protein that was first identified and purified from rabbit skeletal muscle called MAPKAP kinase 2 (Stokoe *et al.*, 1992a). As shown in Figure 1B, the protein MAK-1 is 521 residues in length and contains a protein kinase domain. The kinase domain of human MAPKAP kinase 2 is 53% identical to the kinase domain of nematode MAK-1 (Figure 1B). Mammalian MAPKAP kinase 2 requires phosphorylation by p38 MAP kinase for activity; the sites have been identified (Ben-Levy *et al.*, 1995), and these are conserved in MAK-1. Our analysis of the *C. elegans* proteome reveals that there are two additional MAPKAP kinase 2 paralogues, MAK-2 and MNK-1, which have kinase domains that are 52 and 31% identical to the kinase domain of MAK-1, respectively (Figure 1B).

The Y2H screen identified two independent prey clones for MAK-1 encoding residues 28–521 and 81–521. To further determine a minimal region of MAK-1 required for interaction of twitchin kinase,

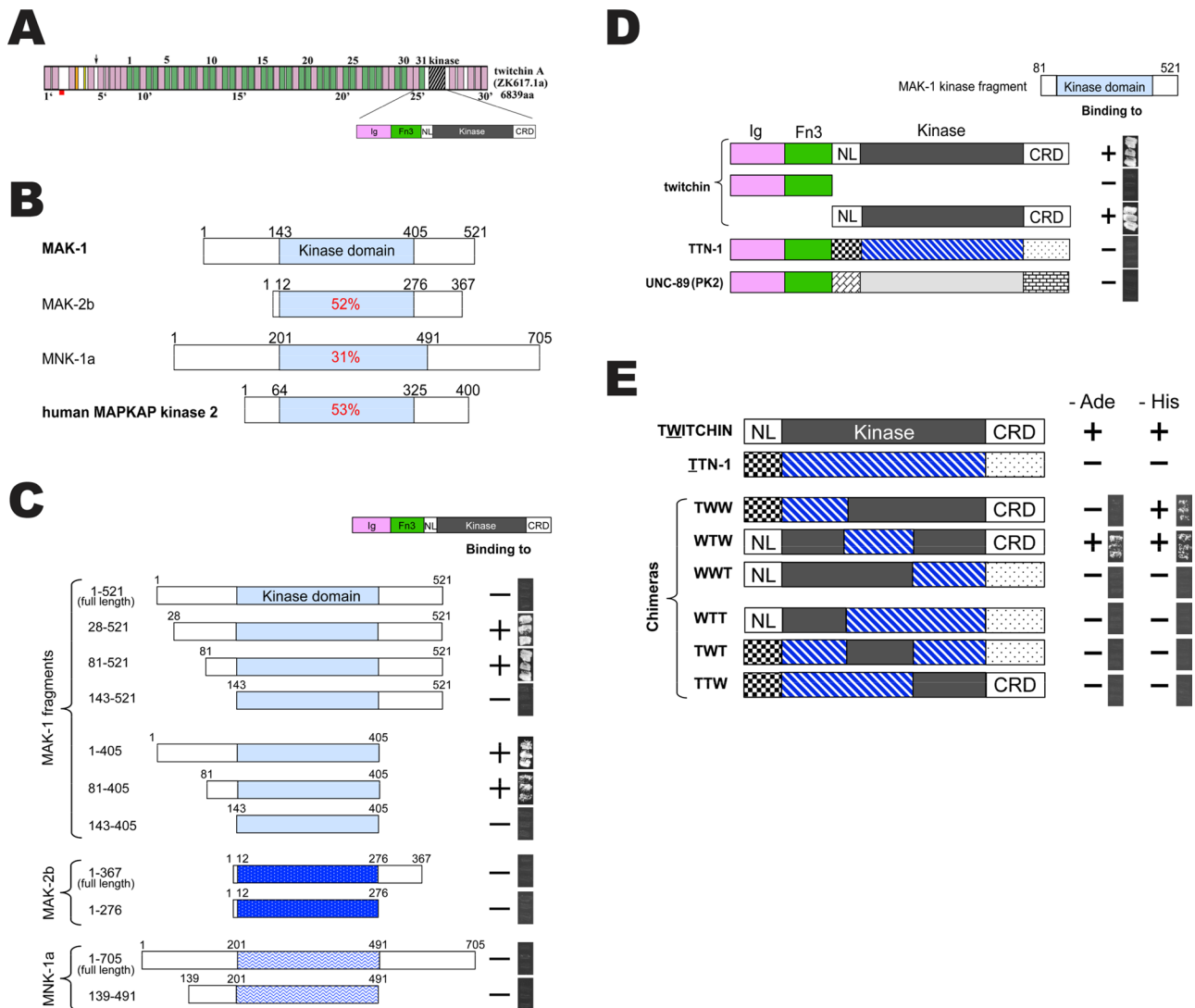


FIGURE 1: Identification of MAK-1 as a binding partner for twitchin kinase. (A) Schematic representation of domains in twitchin, and segment used to search for interacting molecules. Purple, Ig domains; green, Fn3 domains. The Ig25-Fn31-kinase segment of twitchin was used to screen a yeast two-hybrid library, and among the positive preys recovered were two clones representing K08F8.1, later renamed MAK-1 (MAP kinase-associated kinase). (B) Domain organization of MAK-1 and homologous proteins in *C. elegans* and humans. MAK-1 is 521 aa, and the only recognizable domain is a protein kinase domain, most homologous (53% identical) to the protein kinase domain of human MAPKAP kinase 2. The two protein kinases most similar to MAK-1 from *C. elegans* are MAK-2 and MNK-1. The kinase domains of these proteins are, respectively, 52 and 31% identical in sequence to the kinase domain of MAK-1. (C) MAK-1 (81–405) is the minimum region for binding twitchin kinase, and the 2 MAK-1 paralogues do not interact by yeast two-hybrid assays. The indicated segments of MAK-1, MAK-2b, and MNK-1a were tested for interaction with the indicated region of twitchin. (D, E) MAK-1 interacts with twitchin kinase but not two related giant kinases, and the C-terminal region of twitchin kinase is important for binding to MAK-1. (D) By yeast two-hybrid analysis, interaction of MAK-1 with twitchin kinase is specific; the homologous region from the other giant proteins, TTN-1 and UNC-89 (PK2), fail to interact. In addition, the upstream Ig and Fn3 domains of twitchin are not required for interaction with MAK-1. (E) A series of twitchin/TTN-1 chimeras was constructed and assayed for interaction with MAK-1. As indicated, the C-terminal ~140 residues of twitchin, including the end of the kinase catalytic core and most of the CRD, is crucial for this interaction. In C–E, to the right of each row are images of yeast growth of three independent colonies on plates lacking adenine (–Ade; C–E) and on plates lacking histidine (–His; E).

we created deletion derivatives of full-length MAK-1 and used Y2H assays to assess interaction with Ig25-Fn31-NL-Kin-CRD (45 aa). As indicated in Figure 1C, the smallest portion of MAK-1 that interacts with twitchin kinase is MAK-1 (aa 81–405), essentially the kinase catalytic core plus 61 residues of N-terminal sequence. When tested for interaction with twitchin kinase, the MAK-1 paralogues MAK-2 and MNK-1 fail to interact (bottom portions of Figure 1C).

Similarly, by Y2H assays, we determined that the Ig-Fn3 region upstream of twitchin kinase is not required for interaction with MAK-1; interaction was found when the NL-Kin-CRD (45) of twitchin was tested (top three rows of Figure 1D). We next explored the specificity of the interaction of twitchin kinase with MAK-1. In *C. elegans*, there are two additional giant polypeptides with protein kinase domains near their C-termini, TTN-1 and UNC-89. Moreover, the

domain organization upstream of the kinase domains is also conserved, such that all three proteins are organized as Ig-Fn-Kinase. When tested by Y2H assays for interaction with MAK-1, the homologous regions of TTN-1 or UNC-89 PK2 failed to interact (bottom two rows of Figure 1D).

Twitchin CRD is important for binding to MAK-1

Taking advantage of the lack of interaction of TTN-1 with MAK-1 (Figure 1D), we created TTN-1 (“T”) / twitchin (“W”) chimeras and tested them by Y2H to determine which portion of twitchin NL-Kin-CRD (45 aa) is critical for interaction with MAK-1. Analysis of these many chimeras (Figure 1E) suggests that the C-terminal ~140 residues of twitchin, including the end of the kinase catalytic core and most of the CRD, is crucial for this interaction. However, we cannot rule out the possibility that the chimeras that show no interaction are not folded correctly.

To verify the interaction of twitchin kinase with MAK-1 and obtain additional evidence that the C-terminal region of NL-Kin-CRD (60 aa) is important for this interaction, we conducted two types of in vitro binding experiments using purified recombinant proteins. We produced histidine (His)-tagged fragments of twitchin kinase—NL-Kin-CRD (60 aa), Kin-CRD (60 aa), NL-Kin, and Kin—and a maltose-binding protein (MBP) fusion of MAK-1 (81–405). A far-Western assay was conducted in which the twitchin fragments were present on a membrane and incubated with either MBP or MBP-MAK-1 in solution. (A Coomassie-stained gel of 2 µg of each protein used in this experiment is shown in Supplemental Figure S1.) As shown in Figure 2A, the apparent strength of binding depended on the presence of the twitchin CRD (60 aa) region: stronger binding to NL-Kin-CRD (60 aa) and Kin-CRD (60 aa) and weaker binding to NL-Kin and Kin. A pull-down assay was conducted in which the His-tagged fragments of twitchin kinase were incubated in solution with either MBP or MBP-MAK-1 and the proteins pulled down using anti-His antibody conjugated beads; after separation on a gel and transfer to a membrane, MBP-MAK-1 or MBP was detected using anti-MBP. As shown in Figure 2B, only MBP-MAK-1 and not MBP was detected, and the amount of MBP-MAK-1 pulled down was reduced when CRD was missing from the twitchin fragments.

The *mak-1* gene is expressed in body wall muscle, intestine, and hypodermis

Although SAGE data indicate that *mak-1* is expressed in body wall muscle (Meissner *et al.*, 2009; Supplemental Table S1), we sought additional evidence for this expression pattern. A 6.4-kb genomic fragment that includes the putative promoter sequence upstream of *mak-1*, a putative 5′-untranslated region, initiator ATG, and the first 12 nucleotides of coding sequence of *mak-1* was fused to green fluorescent protein (GFP), and transgenic worms carrying this segment were generated. This *mak-1* promoter reporter is expressed in body wall muscle and intestine (Figure 3A), as well as in hypodermis (unpublished data).

mak-1 loss-of-function mutants and generation of specific anti-MAK-1 antibodies

Two *mak-1* intragenic deletion strains were obtained from the *Caenorhabditis* Genetics Center (University of Minnesota, Minneapolis, MN) and the National Bioresource Project (Tokyo, Japan). As depicted on WormBase (www.wormbase.org/species/c_elegans), *mak-1(ok2987)* is a 754–base pair deletion, removing all of exon 3 (Figure 3B). We determined that *mak-1(tm3455)* has both a 7–base pair insertion and a 267–base pair deletion extending from the 3′ end of exon 3 until the 5′ end of intron 4.

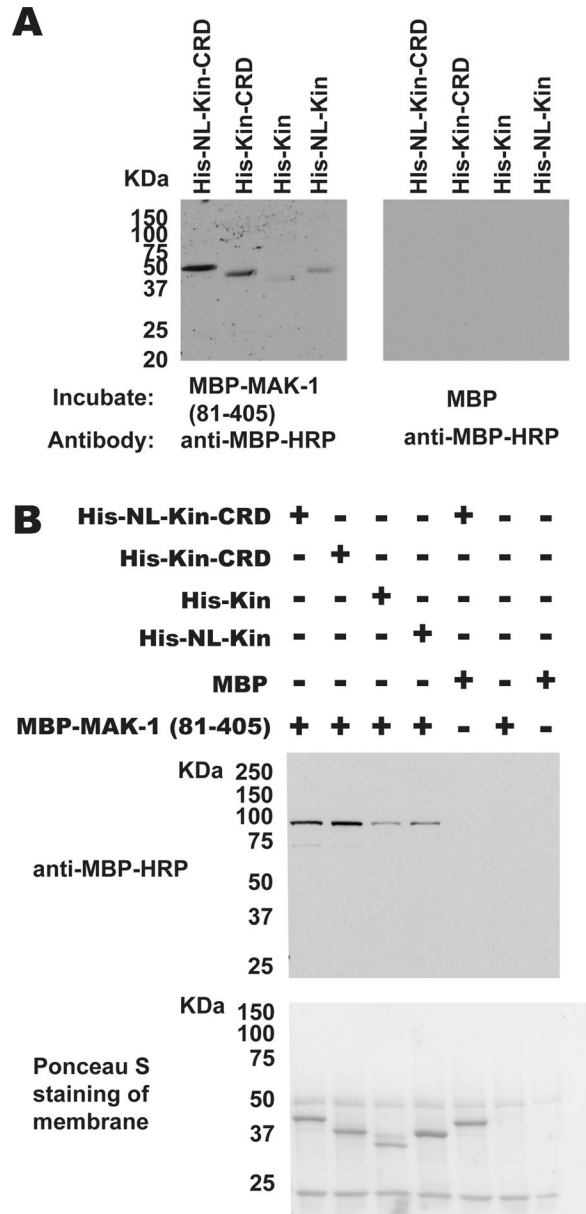


FIGURE 2: Twitchin CRD is important for binding to MAK-1. (A) A far-Western blot was carried out in which the indicated His-tagged fragments of twitchin kinase were separated on a gel, transferred to a blot, and incubated with MBP-MAK-1 or MBP, with binding detected with antibodies to MBP. As shown, MBP-MAK-1 but not MBP binds to the twitchin fragments. However, binding is diminished when the CRD is missing. (B) A pull-down assay was conducted in which the indicated His-tagged fragments of twitchin kinase were incubated in solution with either MBP or MBP-MAK-1 and the proteins pulled down using anti-His antibody–conjugated beads; after separation on a gel and transfer to a membrane, MBP-MAK-1 or MBP was detected using anti-MBP conjugated to HRP and ECL. Note that only MBP-MAK-1 and not MBP was detected, and the amount of MBP-MAK-1 pulled down was diminished when CRD was missing from the twitchin fragments. Below the Western reaction blot is shown the blot stained with Ponceau S before incubation with antibody. The bands at 50 and 25 kDa represent the heavy and light chains of IgG, respectively.

We generated rabbit antibodies to two segments of MAK-1—an N-terminal region (residues 81–142) and a C-terminal region (residues 416–468)—each of them not containing the kinase domain. As shown in Figure 3C, each antibody reacts with a protein of the size

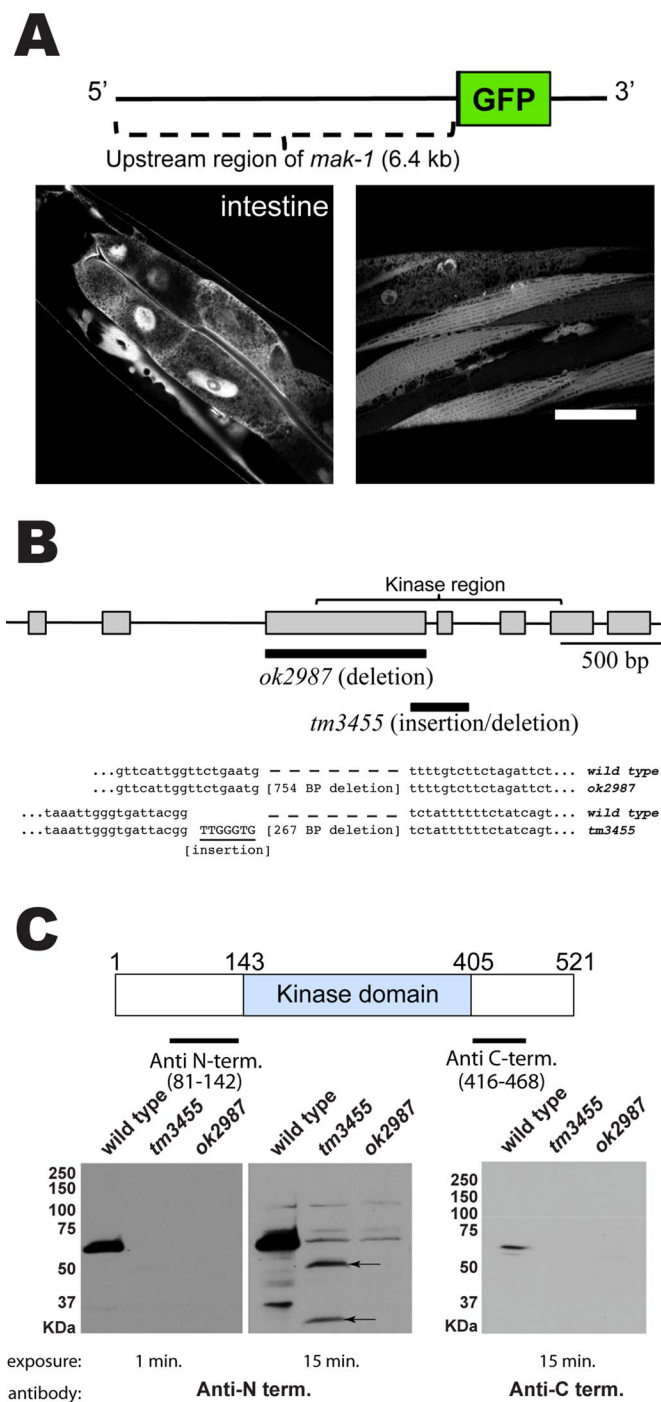


FIGURE 3: *mak-1* expression pattern, mutations, and MAK-1 antibodies. (A) The *mak-1* gene is expressed in the intestine and body wall muscle. To detect *mak-1*-expressing cells, we created transgenic worms expressing GFP from a 6.4-kb segment of genomic DNA upstream of the *mak-1* predicted translational start. GFP was detected in the intestine (left) and body wall muscle cells (right) at the adult stage. Scale bar, 25 μ m. (B, C) *mak-1* mutation sites and effects on MAK-1 protein expression. (B) Schematic representation of the *mak-1* gene, with boxes denoting exons, and introns denoting introns, the approximate spans of each deletion represented, and the sequence alterations shown below. *mak-1(ok2987)* is a 754-base pair deletion, essentially as depicted on WormBase. We determined that *mak-1(tm3455)* has both a 7-base pair insertion and a 267-base pair deletion extending from the 3' end of exon 3 until the 5' end of intron 4. (C) Location of immunogens used to generate antibodies to MAK-1

expected for MAK-1 (~60 kDa) from a wild-type extract on Western blot. For the anti-N-terminal antibody, MAK-1 cannot be detected from the two mutant alleles. On longer exposure, however, two novel bands are detected from *tm3455*, likely representing truncated MAK-1 polypeptides. On longer exposure, no protein is detected from *ok2987*, other than bands found from all three strains likely arising from cross-reactivity to bacterial products. For the anti-C-terminal antibody, MAK-1 proteins cannot be detected even after long exposure time. On the basis of these results, we conclude that *ok2987* is a likely null allele for *mak-1*.

MAK-1 localizes between and around dense bodies and partially colocalizes with MHC B (and, by inference, twitchin) at the edge of the A band

The anti-C-terminal MAK-1 antibody was used to determine whether MAK-1 is localized in the sarcomere and, if so, where it is localized. In immunofluorescence experiments of wild-type body wall muscle, anti-MAK-1 was costained with anti-PAT-6 (α -parvin) to mark the M-lines and dense bodies. As shown in Figure 4A (top row), anti-MAK-1 localizes between and around dense bodies. No signal was obtained with anti-MAK-1 upon staining either *mak-1* mutant animal (Figure 4A, rows 2 and 3), indicating that the localization pattern in wild-type is specific.

Both anti-MAK-1 and all available anti-twitchin antibodies (Moerman *et al.*, 1988; Benian *et al.*, 1996) have been generated in rabbits. Thus we could not costain anti-MAK-1 with anti-twitchin. However, previous studies demonstrate that twitchin colocalizes with MHC B (Moerman *et al.*, 1988), and a mouse monoclonal to MHC B is available (monoclonal 5-8; Miller *et al.*, 1983). Therefore we costained anti-MAK-1 with anti-MHC B. As shown in Figure 4B, some MAK-1 colocalizes with MHC B at the outer edges of the A-band (seen as white dots in the merged image). This result shows that some MAK-1 colocalizes with twitchin, consistent with their interaction *in vivo*.

We next investigated whether loss of function of twitchin would affect the localization of MAK-1. Using two independent *unc-22* alleles, *e66* and *e105*, we observed no obvious difference in the localization of MAK-1 as compared with wild type (Figure 4C).

mak-1 mutants have slightly reduced motility but normal muscle structure

The locomotion of adult *C. elegans* can be assessed by measuring the number of times a worm moves back and forth for a given time in a droplet of liquid (Epstein and Thomson, 1974), often referred to as a "swimming assay." Figure 5A presents swimming assay results for wild type, the two *mak-1* mutants, and three *unc-22* mutants. Although *mak-1(tm3455)* worms show almost the same motility as wild-type worms, *mak-1(ok2987)* worms show slightly reduced motility that is statistically significant. The fact that *ok2987* shows slightly reduced motility but *tm3455* shows normal motility is

and Western blot analysis of wild-type and *mak-1* mutants. Antibodies raised to either an N-terminal or a C-terminal region detect an ~60-kDa protein, the size expected for MAK-1. For the anti-N-terminal antibody, note that on short exposure, MAK-1 cannot be detected from the two mutant alleles. On longer exposure, two novel bands are detected from *tm3455*, likely representing truncated MAK-1 polypeptides (indicated by arrows). On longer exposure, no protein is detected from *ok2987*, other than bands found from all three strains likely arising from cross-reactivity to bacterial products. For the anti-C-terminal antibody, MAK-1 proteins cannot be detected even after long exposure time.

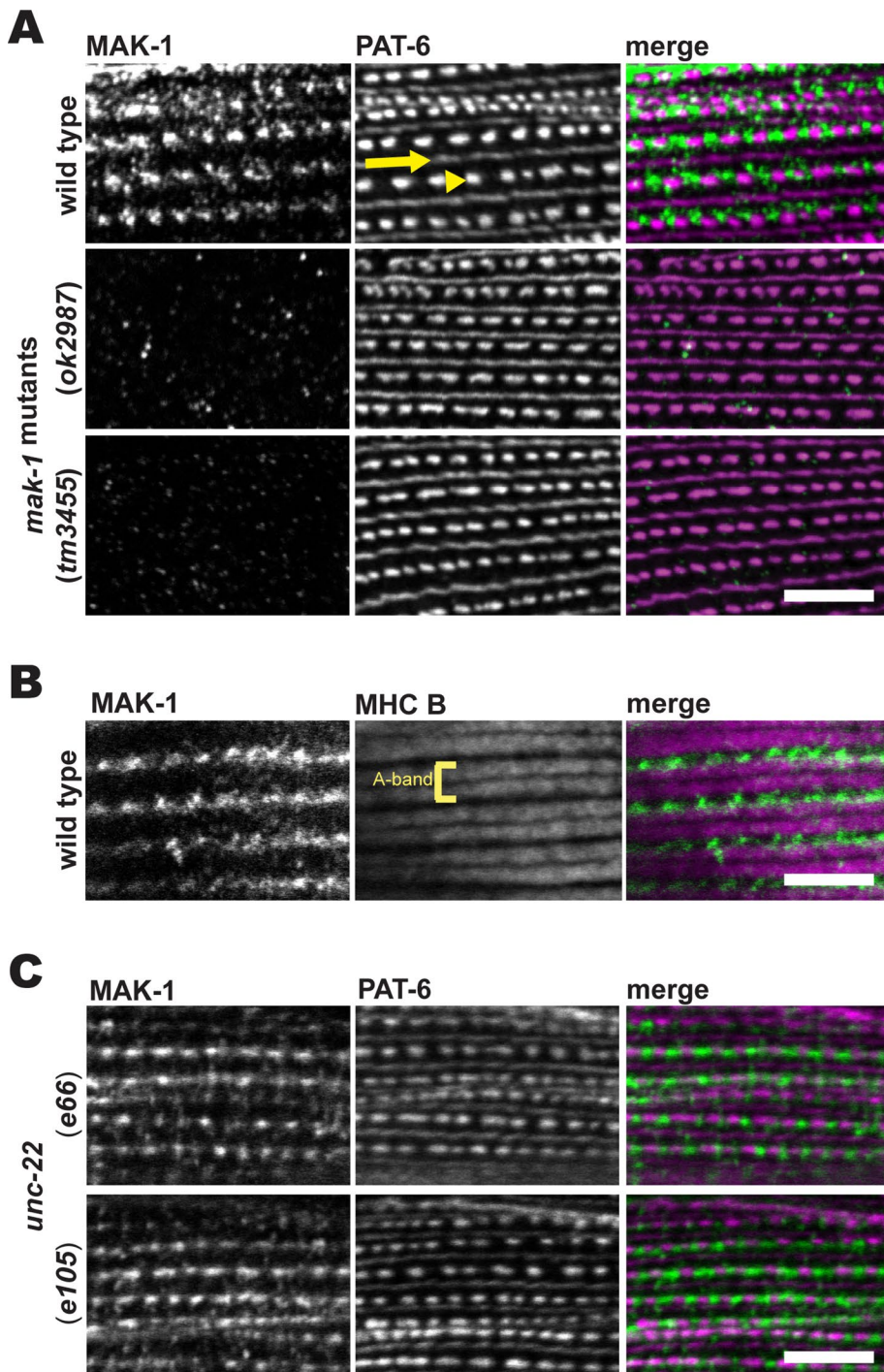


FIGURE 4: Localization of MAK-1 in wild type and in *mak-1* and *unc-22* mutants. (A) Portion of an adult body wall muscle cell from wild type and each of the *mak-1* mutants immunostained with the anti-C-terminal MAK-1 antibody and costained with anti-PAT-6 (α -parvin), which marks M-lines (denoted by an arrow) and dense bodies (denoted by an arrow head). Anti-MAK-1 localizes between and around dense bodies (top) in striated muscle cells. This localization was not detected in *mak-1* mutant animals (middle and bottom). (B) Portion of a wild-type body wall muscle cell immunostained with anti-MAK-1 and anti-MHC B. Anti-MAK-1 partially colocalizes with anti-MHC B at the outer edges of A-bands. (C) Portion of an adult body wall muscle cell from two *unc-22* mutant alleles, *e105* and *e66*, immunostained with anti-MAK-1 and anti-PAT-6. The localization of MAK-1 is not affected by the presence of a mutant form of UNC-22 (twichin). Scale bars, 10 μ m.

consistent with the Western blot results (Figure 3C) indicating that *ok2987* is a likely null allele. For comparison, the *unc-22* null allele, *ct37* (Moerman et al., 1988), and the *unc-22* canonical allele, *e66*,

***mak-1* mutants are partially resistant to nicotine**

Nicotine is an acetylcholine agonist, and when wild-type animals are exposed to a solution of nicotine, they become paralyzed (i.e., they

are much slower than wild type. Of interest, *unc-22(e105)* shows slightly increased locomotion (Figure 5A).

Given that *mak-1(ok2987)* has a slightly reduced motility, we expected that there might be some defect in the organization of its sarcomeres. To examine this possibility, we conducted immunofluorescence localization of various sarcomere proteins in wild type and *mak-1(ok2987)*. In addition to twitchin, we assessed the localization of an ECM component, UNC-52(perlecan), the M-line and dense body proteins UNC-112 (kindlin) and UNC-95, and the dense body protein ATN-1 (α -actinin), the M-line protein UNC-89 (obscurin), and MHC A (a myosin heavy chain isoform that lies in the middle of thick filaments). Antibodies to all these proteins showed normal localization in *mak-1(ok2987)* mutant muscle (Figure 5B). Thus we can attribute the slightly reduced motility of *mak-1(ok2987)* to a possible defect in regulation of muscle contraction rather than a defect in sarcomere organization.

Sarcomeres are disorganized in *unc-22(e66)* but normal in *unc-22(e105)*

There are many available mutant alleles for *unc-22*. Although some alleles, such as the null *ct37* or the amber allele *s32*, are very slow moving, other alleles, such as *e105*, show near-normal motility (Moerman et al., 1988). Despite this variation in locomotion defects, all alleles “twitch”—that is, shallow bends occur in multiple places along the surface of the animal one to several times per second, whether the animal is stationary or moving in its usual snake-like locomotion. Given that our swimming assays showed reduced motility for *e66* and increased motility for *e105*, we wondered how sarcomere organization would be affected. Figure 6 presents immunostaining results using antibodies to a battery of sarcomeric proteins. In *unc-22(e66)* muscle, all of these proteins display abnormal localization. In contrast, in *unc-22(e105)* muscle, all of these proteins show normal localization. Therefore a mild allele of *unc-22*, *e105*, and a null allele of *mak-1*, *ok2987*, each displays normal sarcomere organization. Our interpretation is that at least one function of UNC-22 (twichin), and the main function of MAK-1, is in regulating muscle contraction. However, it is also possible that MAK-1 does have a role in sarcomere organization, but our immunostaining did not detect subtle defects in *mak-1(ok2987)*.

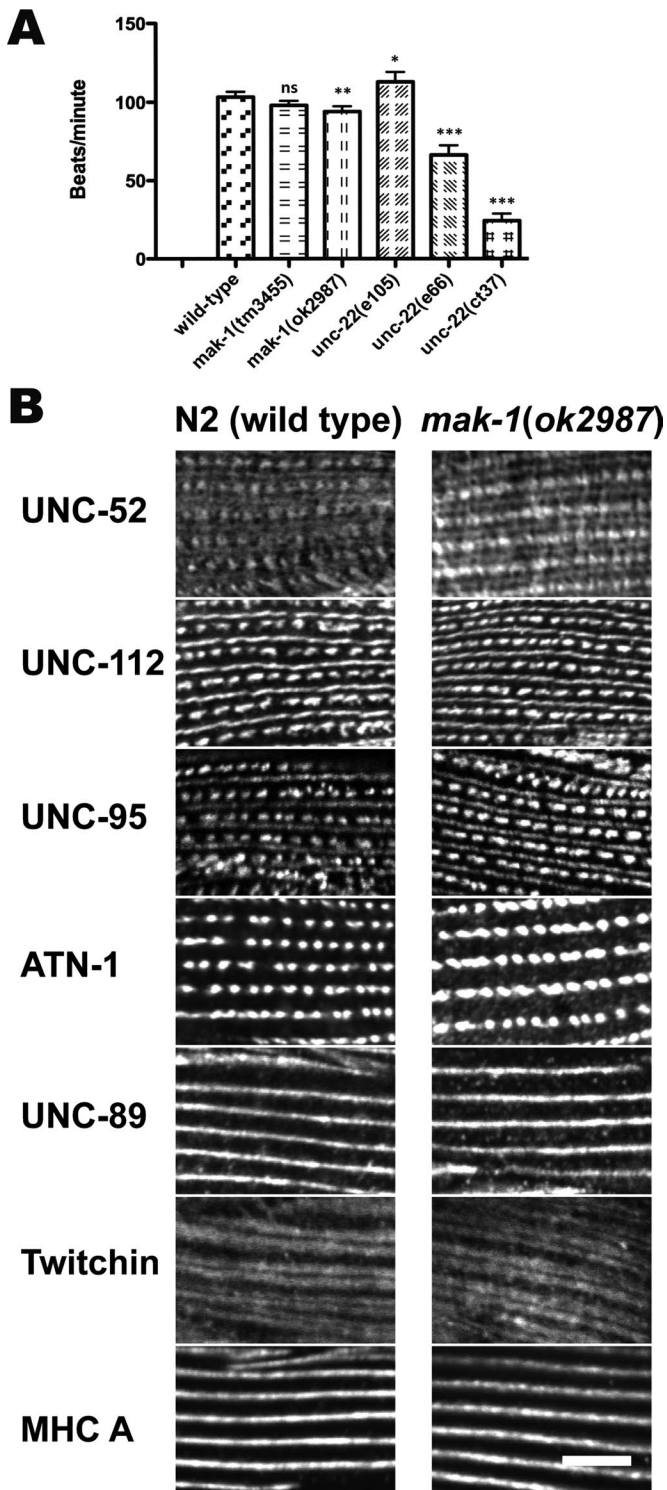


FIGURE 5: Phenotype of *mak-1* mutants. (A) A *mak-1* mutant has slightly reduced locomotion. Results of swimming assays on adult nematodes of the indicated genotypes. Data are means and SEs with $n = 20$. Although *mak-1(tm3445)* animals show almost the same motility as wild-type animals, *mak-1(ok2987)* animals show slightly reduced motility that is statistically significant. The *unc-22*-null allele, *ct37*, and the *unc-22* canonical allele, *e66*, are much slower than wild type. In contrast, *unc-22(e105)* shows normal or even increased locomotion in this assay. (B) *mak-1(ok2987)* shows normal sarcomeric structure. Images show part of a body wall muscle cell from either wild type or *mak-1(ok2987)* immunostained with the indicated antibodies. UNC-52 (perlecan), UNC-112, and UNC-95 all localize to

are sensitive). When *unc-22* mutants are exposed to nicotine, however, they continue to move and twitch violently (i.e., they are resistant; Moerman *et al.*, 1988). We used an automated device, the WMicrotracker, to monitor the locomotion of multiple worms in a microtiter dish over time upon exposure to a solution of 0.1 or 0.05% nicotine. As shown in Figure 7A, ~90% of wild-type animals stop moving after ~30 min. However, *unc-22* mutants, regardless of allele, continue moving, even after 60 min. Of interest, as shown in Figure 7B, *mak-1* mutants show an intermediate response, that is, they are partially resistant. The likely null allele, *mak-1(ok2987)*, shows greater resistance than *mak-1(tm3445)*, and this effect is shown in either 0.1 or 0.05% nicotine (Figure 7C). Because both *unc-22* and *mak-1* mutants show an abnormal response to nicotine, we wondered how the double mutant might respond. We fed wild-type and *mak-1(ok2987)* worms bacteria expressing double-stranded RNA for *unc-22* to knock down *unc-22* mRNA. As indicated in Figure 7D, the double mutant *mak-1(ok2987); unc-22(RNAi)* shows complete resistance, just like *unc-22(RNAi)*. That is, *unc-22* is epistatic to *mak-1*.

The *mak-1* paralogues *mnk-1* and *mak-2* are also expressed in body wall muscle

We wondered whether loss of function of either or both of the *mak-1* paralogues *mnk-1* or *mak-2* might also show a phenotype similar to *mak-1*, that is, partial resistance to nicotine. Before examining this question, we wanted to know whether *mnk-1* and *mak-2* are even expressed in adult body wall muscle. Thus we created transgenic animals that express GFP from genomic segments upstream of the putative start sites for *mnk-1* or *mak-2*. WormBase indicates two predicted isoforms of *mnk-1*, *mnk-1a* and *mnk-1b*, which differ in their 5'-most exons, suggesting the existence of two different promoters. We examined the expression patterns of transgenic worms expressing GFP driven by sequences upstream of each of these alternative 5'-most exons. As shown in Figure 8A, *mnk-1a* and *mnk-1b* are expressed in the same tissues/organs: the pharynx, the intestine, the vulval muscles, and body wall muscle. The promoter for *mak-2* is expressed in the pharynx, the intestine, and body wall muscle (Figure 8B).

mnk-1, *mak-2*, *pmk-1*, and *pmk-3* are all partially resistant to nicotine

Using the same WMicrotracker assays, we found that *mnk-1* and *mak-2* are partially resistant to nicotine (Figure 9, A and B), and their resistance is in the order *mak-1* > *mak-2* > *mnk-1*. We also examined the nicotine response of the double mutants *mak-1; mak-2* and *mak-1; mnk-1*. The *mak-1; mak-2* mutant showed more resistance than *mak-1* alone (Figure 9, C and D) but less resistance than *unc-22(e105)* (Figure 9, E and F). These results suggest that *mak-1* and *mak-2* contribute to nicotine resistance in the same pathway, but other unidentified players are probably also involved. As noted, mammalian MAPKAP kinase 2 is phosphorylated, and activated, by p38 MAP kinase. *C. elegans* has three p38 MAP kinases, encoded

M-lines and dense bodies; UNC-52 in the extracellular matrix; and UNC-112 and UNC-95 in the muscle cytoplasm close to the cell membrane. ATN-1 (α -actinin) localizes to the main, deeper portion of the dense bodies. UNC-89 (obscurin) is located at M-lines full depth, from muscle cell membrane, up through the deepest part of the myofibrillar lattice. Twitchin localizes to the outer portions of A-bands, and MHC A localizes to the middle of A-bands. For all these proteins, localization is no different in *mak-1(ok2987)* muscle than in wild-type muscle. Scale bar, 10 μ m.

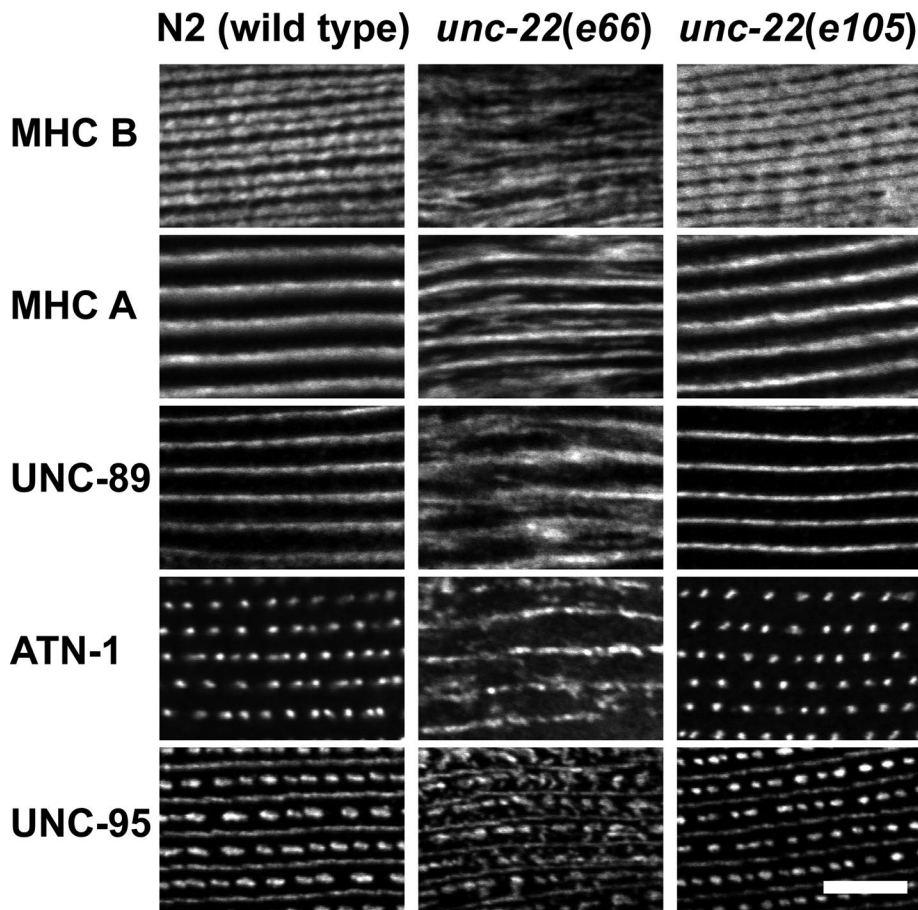


FIGURE 6: Sarcomeres are disorganized in *unc-22(e66)* but normal in *unc-22(e105)*. Each image shows part of a body wall muscle cell from wild type, *unc-22(e66)*, or *unc-22(e105)*. Some of the same antibodies described in Figure 8 were used, and, in addition, antibodies to MHC B, which localizes to the outer portions of A-bands. In *unc-22(e66)* muscle, all of these proteins show abnormal localization as compared with wild type. In *unc-22(e105)*, all of these proteins show normal localization. Scale bar, 10 μ m.

by separate genes that are organized into a single operon in the order *pmk-3*, *pmk-2*, and *pmk-1* (Berman *et al.*, 2001). SAGE data suggest that *pmk-3*, *-2*, and *-1*, like *mak-1*, are also expressed in body wall muscle (Meissner *et al.*, 2009). Although an intragenic deletion of *pmk-2* is lethal at the L1 stage, this phenotype is not related to the disruption of the *pmk-2* gene (Berman *et al.*, 2001). This lethality prevented our analysis using the WMicrotracker. However, as shown in Figure 9, G and H, loss of function of either *pmk-1* or *pmk-3* results in partial nicotine resistance, each fairly similar to *mak-1*. This result is at least consistent with *pmk-1* and *pmk-3* being part of the same genetic pathway as *mak-1*.

MAK-1 can phosphorylate twitchin kinase in vitro

Given that our results indicate that MAK-1 and twitchin interact both physically and genetically and have overlapping mutant phenotypes, we explored the enzyme/substrate relationship of these two protein kinases. First, we used as source of kinase the minimum portion of MAK-1, residues 81–405, which interacts with twitchin and is predicted to contain an intact protein kinase domain. As source of substrate, we used twitchin NL-Kin-CRD, in which the highly conserved lysine (lysine 185 in von Castelmur *et al.*, 2012; lysine 6290 in UNC-22b [WormBase]) was converted to alanine. This lysine is known in other kinases to coordinate ATP, and when mutated to alanine or several other amino acids, it will inactivate the kinase

(Iyer *et al.*, 2005). Thus recombinant His-tagged MAK-1(81–405) and twitchin NL-Kin-CRD (K to A) were used in in vitro protein kinase assays. As shown in Figure 10A, as expected, NL-Kin-CRD (K to A) showed no autophosphorylation. In contrast, MAK-1(81–405) did show autophosphorylation, and, of greater importance, was able to phosphorylate twitchin NL-Kin-CRD (K to A). Because our twitchin/TTN-1 chimeras in Y2H assays and in vitro binding assays indicate that twitchin's CRD is important for binding to MAK-1, we wondered whether in vitro kinase assays could show that the CRD is phosphorylated by MAK-1. We tested a series of deletion derivatives of NL-Kin-CRD (K to A) as substrates. As shown in Figure 10B, the only fragment that showed unambiguous phosphorylation was the intact NL-Kin-CRD. Using the same type of assay, we looked for phosphorylation of MAK-1 in which MAK-1 was predicted to be catalytically inactive (converting lysine 173 to alanine), using fully active twitchin kinase (the kinase domain itself; von Castelmur *et al.*, 2012). In this experiment, we did not observe phosphorylation of MAK-1 (K to A) by twitchin kinase (unpublished data).

DISCUSSION

We discovered that the twitchin kinase domain interacts with another protein kinase, the nematode orthologue of MAPKAP kinase 2, MAK-1. For each protein, the minimal necessary sequence includes the kinase catalytic core plus some flanking sequence; for MAK-1, it is the catalytic core plus 62 residues N-terminal (Figure 1C); for twitchin kinase, it is NL plus catalytic core plus 45 of 60 residues of the CRD (Figure 1D). Both yeast two-hybrid assays using twitchin/TTN-1 chimeras (Figure 1E) and in vitro binding assays using purified recombinant deletion derivatives of twitchin NL-Kin-CRD (Figure 2) indicate that the CRD is crucial for this interaction. Of interest, a sequence in the second protein kinase domain of UNC-89 (PK2) in the analogous position of the CRD of twitchin is also required for interaction with SCPL-1, a CTD-type protein phosphatase (Qadota *et al.*, 2008).

We further demonstrate that the *mak-1* promoter is expressed in body wall muscle (Figure 3A) and that antibodies to MAK-1 detect a protein of appropriate size from nematode extracts (Figure 3C) that localizes in the sarcomere around and between dense bodies with some overlap with the A-band localization of twitchin (Figure 4, A and B). We characterized the phenotype of two loss-of-function *mak-1*–mutant alleles (Figure 3B). *mak-1(ok2987)* shows a slight decrease in worm locomotion (Figure 5A) and no effect on sarcomere organization (Figure 5B). We also found that *unc-22(e105)*, although showing the expected “twitching phenotype,” shows no defects in sarcomere organization (Figure 6). Both *unc-22* and *mak-1* mutants have an abnormal response to nicotine; *unc-22* mutants, regardless of the strength of the allele, showed complete resistance to nicotine, whereas *mak-1* mutants showed partial resistance to nicotine (Figure 7). An *unc-22; mak-1* double mutant showed complete

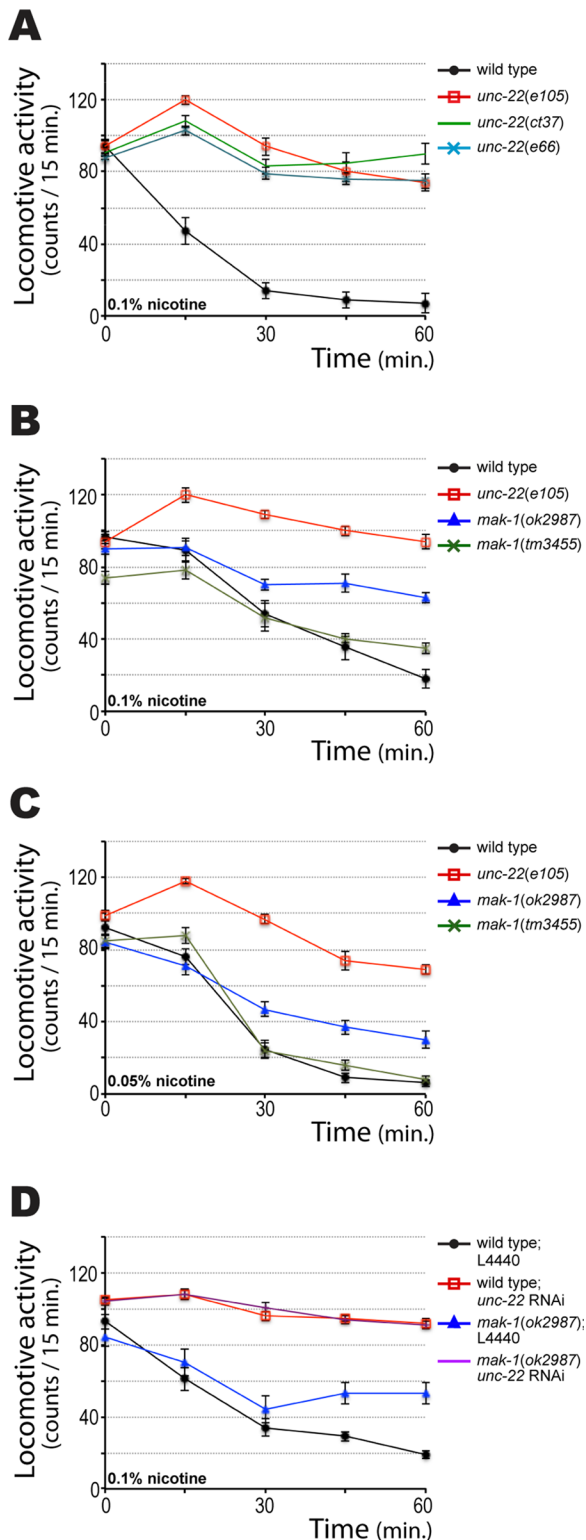


FIGURE 7: Response of wild-type, *unc-22*, and *mak-1* mutant strains to nicotine. A device called a WMicrotracker (DesignPlus) was used to monitor the locomotion of multiple worms per well in a microtiter dish over time during exposure to a solution of 0.1 or 0.05% nicotine. (A) Response of wild-type and three *unc-22*-mutant alleles. In 0.1% nicotine, wild-type animals nearly stop moving by 30 min. In contrast, *unc-22*-mutant animals, regardless of allele, continue moving even after 60 min. (B) Response of wild-type, *unc-22(e105)*, and two *mak-1*-mutant alleles. In 0.1% nicotine, after 60 min of exposure, wild-type animals stop moving, whereas *unc-22(e105)* animals

resistance (Figure 7D), indicating that *unc-22* is epistatic to or genetically downstream of *mak-1*. Two *mak-1* paralogues, *mak-2* and *mnk-1*, also are expressed in body wall muscle (Figure 8), and each showed partial but less resistance to nicotine than *mak-1* (Figure 9, A–F). Loss of function of each of two of the three p38 MAP kinases in *C. elegans* showed partial resistance to nicotine (Figure 9, G and H). These data suggest that *pmk-1*, *pmk-3*, *mak-2*, and *mnk-1* are part of the same pathway as *mak-1* and twitchin (Figure 11).

unc-22(e105) has a fascinating phenotype. Although, like all known *unc-22*-mutant alleles, it twitches and is resistant to nicotine (Figure 7), it shows *normal* (Figure 6) rather than abnormal muscle structure and *increased* rather than decreased motility in swimming assays (Figure 5A). *unc-22(e105)* is a missense mutation in the seventh Ig domain of twitchin, changing a highly conserved glycine to an arginine, and results in normally localized twitchin by immunostaining (unpublished data). Studies in *Aplysia* and *Mytilus* suggest that the normal function of twitchin is to inhibit the rate of relaxation (Probst et al., 1994; Siegman et al., 1998; Funabara et al., 2007). If this same physiological function for twitchin pertains to *C. elegans* muscle, then in *unc-22(e105)*, reduced inhibition of relaxation (i.e., faster relaxation time) might result in an overall faster contraction/relaxation cycle and thus faster worm locomotion.

Our results suggest that MAK-1 is an activator of twitchin kinase. This is suggested by the finding that the CRD of twitchin kinase is crucial for this interaction and because the CRD is one of two flanking sequences (the other being NL) that independently inhibit twitchin kinase activity in vitro (von Castelmur et al., 2012). Although molecular dynamics simulations of the twitchin Fn-NL-kinase-CRD-Ig segment show that pulling force removes the NL inhibitor, the CRD inhibitor remains attached to the kinase catalytic core. We suggest that pulling force removes the NL and activates the kinase to half-maximal activity and that full activation occurs when MAK-1 interacts with or possibly phosphorylates the CRD (Figure 11). Alternatively, partial activation by mechanical force and partial activation by MAK-1 occur independently according to different physiological demands. One interpretation of our genetic epistasis experiment is that twitchin kinase is downstream of MAK-1, and one possibility is that MAK-1 phosphorylates twitchin kinase in or near the CRD. Consistent with this hypothesis, in in vitro protein kinase assays, we can show that MAK-1 phosphorylates twitchin NL-Kin-CRD (Figure 10A), but the reciprocal experiment failed to show that twitchin kinase can phosphorylate MAK-1 (unpublished data). To roughly map the phosphorylation site(s), we tested Kin-CRD, Kin, and NL-Kin, but we could only unambiguously demonstrate that the intact NL-Kin-CRD was phosphorylated (the twitchin fragments ran too closely to the position of MAK-1 on the gel). Further experiments are needed to address the questions of phosphorylation sites, whether phosphorylation by MAK-1 activates twitchin kinase catalytic activity, and whether this phosphorylation and/or activation occurs in vivo.

continue to move. *mak-1(ok2987)*, the putative null allele of *mak-1*, but not *mak-1(tm3445)*, shows an intermediate response; that is, *ok2987* is partially resistant to nicotine. (C) At a slightly lower concentration of nicotine (0.05%), even *mak-1(tm3445)* shows partial resistance to nicotine. (D) In 0.1% nicotine, wild-type animals fed bacteria with an empty RNAi plasmid stop moving, but wild-type animals fed bacteria with an *unc-22(RNAi)* plasmid continue to move after 60 min exposure. Whereas *mak-1(ok2987)* animals fed bacteria with an empty RNAi plasmid show an intermediate response, *mak-1(ok2987)* animals fed bacteria with an *unc-22 RNAi* plasmid continue to move. Therefore *unc-22* is epistatic to *mak-1*.

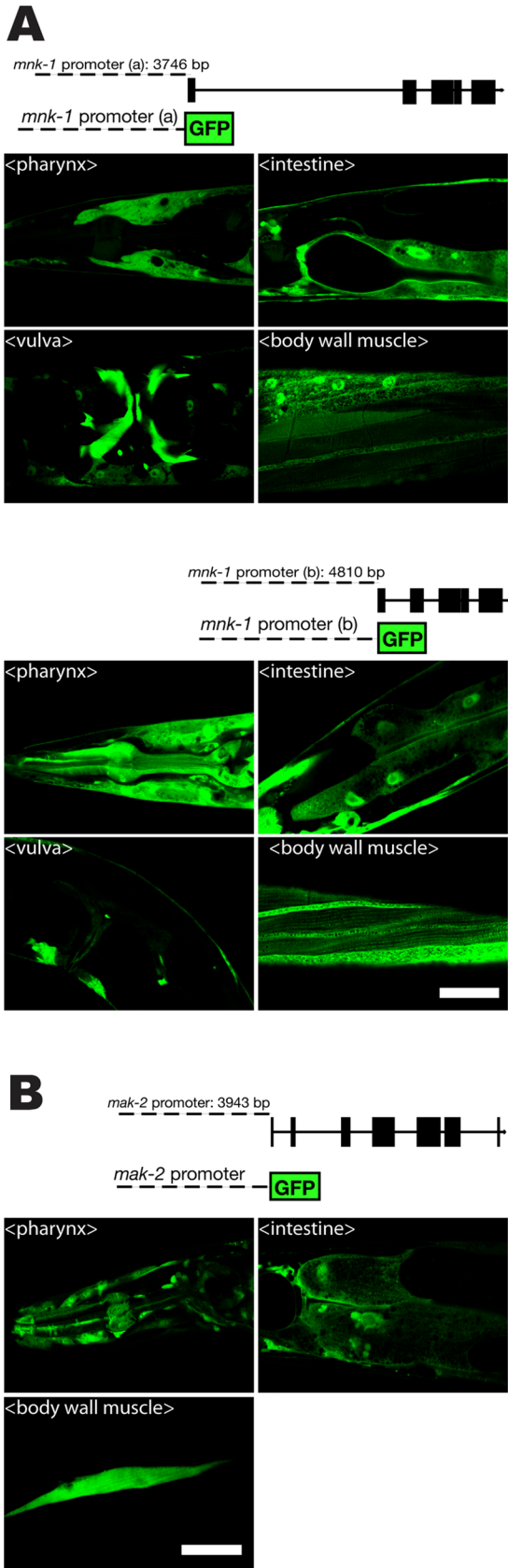


FIGURE 8: Adult expression patterns of *mnk-1* and *mak-2* promoters. (A) On WormBase there are two predicted *mnk-1* splicing patterns, *mnk-1a* and *mnk-1b*. To detect *mnk-1a*-expressing cells, transgenic worms were created that express GFP from a 3.7-kb segment of

Although our data suggest that MAK-1 phosphorylates twitchin kinase, there could be additional substrates. Quite different substrates have been putatively identified for mammalian MAPKAP kinase 2. In vitro, MAPKAP kinase 2 phosphorylates mouse heat shock protein 25 (hsp25) and human heat shock protein 27 (hsp27); fractionation of rabbit skeletal muscle proteins reveals that hsp25 kinase activity copurifies with MAPKAP kinase 2 activity (Stokoe *et al.*, 1992b). Of interest, in *C. elegans*, one of the small heat shock proteins, hsp25, localizes to sarcomeric dense bodies and M-lines (near the localization of MAK-1) and has been shown to exist in a complex with the dense body components vinculin and α -actinin (Ding and Candido, 2000), so there is a possibility that these proteins could also be substrates for MAK-1 in vivo.

We postulate that MAK-1 is part of a cascade that involves p38 and twitchin kinase to regulate muscle contractile activity. Because mammalian p38 and MAPKAP kinase 2 are activated by and respond to intracellular stress, perhaps the model we propose, at least in *C. elegans*, provides a mechanism by which muscle activity is adjusted in response to stress. MAPKAP kinase 2 is involved in stress-activated signaling in heart muscle: MAPKAP kinase 2 is highly expressed in the human heart; in cultured rat cardiac muscle cells, there is increased MAPKAP kinase 2 activity and phosphorylation of hsp25 in response to experimental stressors—heat shock, hydrogen peroxide, or phorbol ester exposure (Zu *et al.*, 1997). A “stress” that could be encountered in vivo is ischemia/hypoxia: MAPKAP kinase 2 activity is increased during ischemia in “preconditioned” rabbit hearts (Nakano *et al.*, 2000). A MAPKAP kinase 2-mediated stress response may not be beneficial: Shiroto *et al.* (2005) report that ischemia/reperfusion of the mouse heart leads to activation of both p38 and MAPKAP kinase 2; a mouse that carries a knockout of MAPKAP kinase 2 is resistant to injury after ischemia/reperfusion, including a decreased number of apoptotic cardiomyocytes.

We also postulate that our putative p38/MAK-1/twitchin kinase cascade (Figure 11) results in inhibition of muscle relaxation. Support for this idea comes from recent studies of mouse skeletal muscle: Scharf *et al.* (2013) report that a MAPKAP kinase 2 and MAPKAP kinase 3 double-knockout mouse shows enhanced expression of the slow oxidative skeletal muscle gene program; use of reporter gene and electrophoretic mobility shift assays demonstrates that MAPKAP kinase 2 catalytic activity directly regulates the promoters of fast fiber myosin heavy chain and slow fiber SERCA2; moreover, there is accelerated relaxation and enhanced contractility of cardiomyocytes and improved force parameters of skeletal muscle.

The abnormal response of *mak-1* mutants to nicotine may be mechanistically related to a finding about MAPKAP kinase 2 in mammalian smooth muscle. Carbachol is a muscarinic acetylcholine agonist. When canine airway smooth muscle is exposed to carbachol, increased phosphorylation of recombinant hsp27 results (Larsen, 1997).

genomic DNA upstream of the *mnk-1a* predicted translational start. GFP was detected in the pharynx, intestine, vulva muscle, and body wall muscle at the adult stage. To detect *mnk-1b*-expressing cells, transgenic worms were made that expressed GFP from a 4.8-kb segment of DNA upstream of the *mnk-1b* translational start. GFP was detected in the pharynx, including pharyngeal muscle, intestine, vulva muscle, and body wall muscle. (B) To detect *mak-2*-expressing cells, transgenic worms were made that expressed GFP from a 3.9-kb genomic segment upstream of the *mak-2* predicted translational start. Expression was detected in pharynx, intestine, and body wall muscle. Scale bar, 25 μ m.

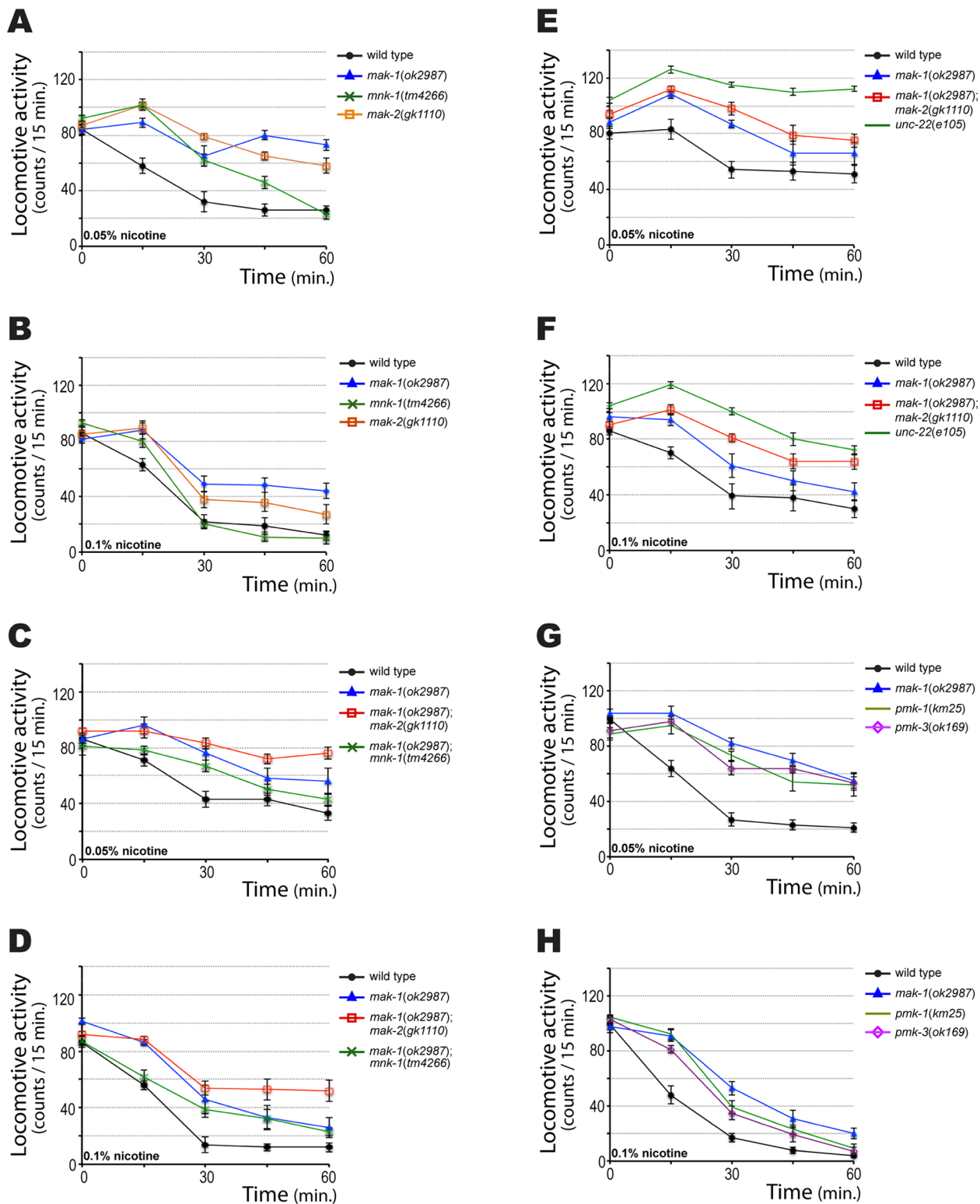


FIGURE 9: Response of *mnk-1*, *mak-2*, *pmk-1*, and *pmk-3* mutants to nicotine. The WMicrotracker was used monitor the locomotion of the indicated strains to the indicated concentrations of nicotine. (A, B) Response of wild type, *mak-1(ok2987)*, *mnk-1(tm4266)*, and *mak-2(gk1110)* to 0.05 and 0.1% nicotine, respectively. Note that *mnk-1* and *mak-2* are partially resistant to nicotine, although to a lesser extent than *mak-1*. (C, D) Response of wild type and *mak-1*, *mak-1; mak-2* and *mak-1; mnk-1* double mutants to 0.05 and 0.1% nicotine, respectively. Note that the *mak-1; mak-2* double mutant shows enhanced resistance compared with either *mak-1* alone or the *mak-1; mnk-1* double mutant. (E, F) Response of wild type, *mak-1*, the *mak-1; mak-2* double, and *unc-22(e105)* to 0.05 and 0.1% nicotine, respectively. Although the *mak-1; mak-2* double is more resistant than *mak-1*, it is less resistant than *unc-22(e105)*. (G, H) Response of wild type, *mak-1*, *pmk-1(km25)*, and *pmk-3(ok169)* to 0.05 and 0.1% nicotine, respectively. *pmk-1* and *pmk-3* are also partially resistant but consistently less resistant than *mak-1*.

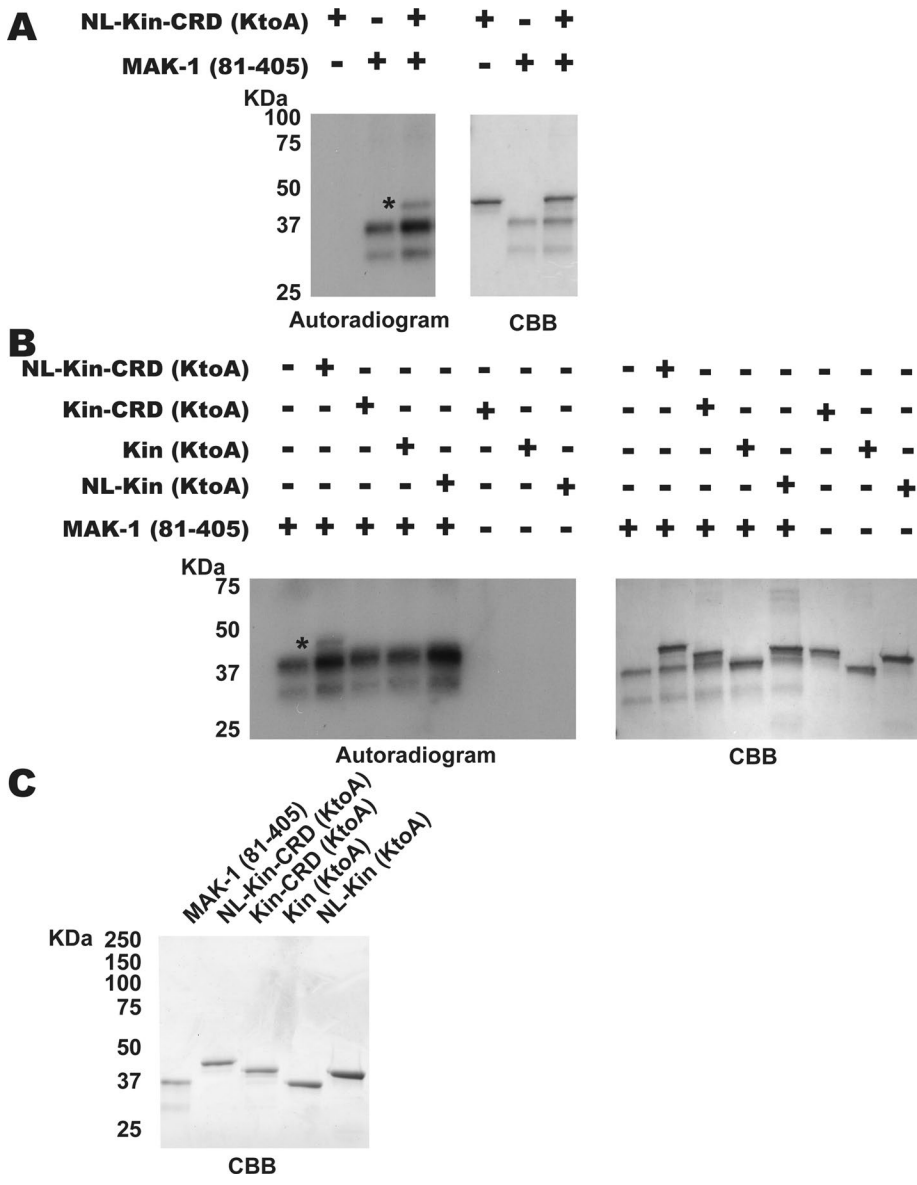


FIGURE 10: MAK-1 phosphorylates twitchin kinase in vitro. (A) A protein kinase assay was conducted using MAK-1 (81–405) as the source of kinase and catalytically dead (K to A) twitchin NL-Kin-CRD as substrate. As expected, NL-Kin-CRD (K to A) does not show autophosphorylation (on autoradiogram, first lane from the left). However, MAK-1 (81–405) shows autophosphorylation (second lane from the left), and MAK-1 phosphorylates NL-Kin-CRD (K to A; third lane from the left, indicated with an asterisk). (B) Protein kinase assays were conducted using MAK-1 (81–405) as the source of kinase and various deletion derivatives of twitchin NL-Kin-CRD (K to A) as substrate. As shown by an asterisk, only NL-Kin-CRD was phosphorylated. For A and B the autoradiogram is shown on the left, and the Coomassie brilliant blue (CBB)–stained gel is shown on the right. (C) SDS–PAGE of 2 μ g each of the proteins used in the kinase assays, stained with CBB. Each protein has an N-terminal hexahistidine tag. The positions of molecular weight markers are indicated.

Finally, we found that the promoters for *mak-1* and its paralogues *mnk-1* and *mak-2* are expressed not just in muscle; they are also expressed in the intestine. Similarly, the p38 kinases are expressed in body wall muscle and the intestine, based on SAGE analysis (Meissner *et al.*, 2009), and in the intestine based on promoter analysis (Berman *et al.*, 2001). The function of intestinal expression is unknown, but may involve stress response: in *Drosophila*, a complex of p38 and MAPKAP kinase 2 is required to prevent stress-dependent damage to intestinal epithelial cells;

impaired p38/MAPKAP kinase 2 signaling leads to apoptosis of intestinal epithelial cells and subsequent loss of hindgut epithelial integrity (Seisenbacher *et al.*, 2011).

MATERIALS AND METHODS

Screening of yeast two-hybrid library

A twitchin bait plasmid containing Ig25-Fn32-Kinase-CRD (45 aa) (Qadota *et al.*, 2008) was used for screening a *C. elegans* yeast two-hybrid cDNA library (RB2, a gift from Robert Barstead, Oklahoma Medical Research Foundation, Oklahoma City, OK). The screening procedure was described previously (Miller *et al.*, 2006). Yeast two-hybrid assays were conducted as described in Mackinnon *et al.* (2002).

Deletion derivatives of MAK-1 and twitchin

cDNA fragments from MAK-1 and twitchin were amplified by PCR (primers: YHM1–YHM5, YHM13–YHM15, and TWI-F; see Supplemental Table S2) and cloned into pBluescript and then confirmed by DNA sequencing. Error-free fragments were transferred into yeast two-hybrid vectors (MAK-1 fragments into pGAD, prey; twitchin fragments into pGBDU, bait).

Cloning of MAK-2 and MNK-1

cDNA fragments of MAK-2 and MNK-1 were amplified by PCR (primers: YHM6–YHM12) from the RB2 library. Amplified fragments were first cloned into pBluescript. After confirmation of DNA sequences, error-free fragments were cloned into pGAD, the yeast two-hybrid prey vector.

Construction of twitchin/TTN-1 chimeras

Chimeric fragments were created by PCR (primers: YHM15–YHM21) using chimeric primers and twitchin and TTN-1 cDNAs (Qadota *et al.*, 2008) according to a protocol described previously (Qadota *et al.*, 1994). Error-free fragments were placed into pGAD, the yeast two-hybrid prey vector.

In vitro binding assays with purified recombinant proteins

The expression of His-tagged twitchin kinase fragments containing the kinase catalytic core were described previously (von Castelmur *et al.*, 2012). For expression of MBP-MAK-1 (81–405), the corresponding MAK-1 cDNA fragment (PCR amplified with primers YHM4 and YHM5) was cloned into pMAL-KK-1 (a gift from Kozo Kaibuchi, Nagoya University, Nagoya, Japan). His-tagged twitchin kinase fragments and MBP-MAK-1 (81–405) were purified as described previously (Mercer *et al.*, 2006). A far-Western assay was conducted as follows: 1 μ g of each

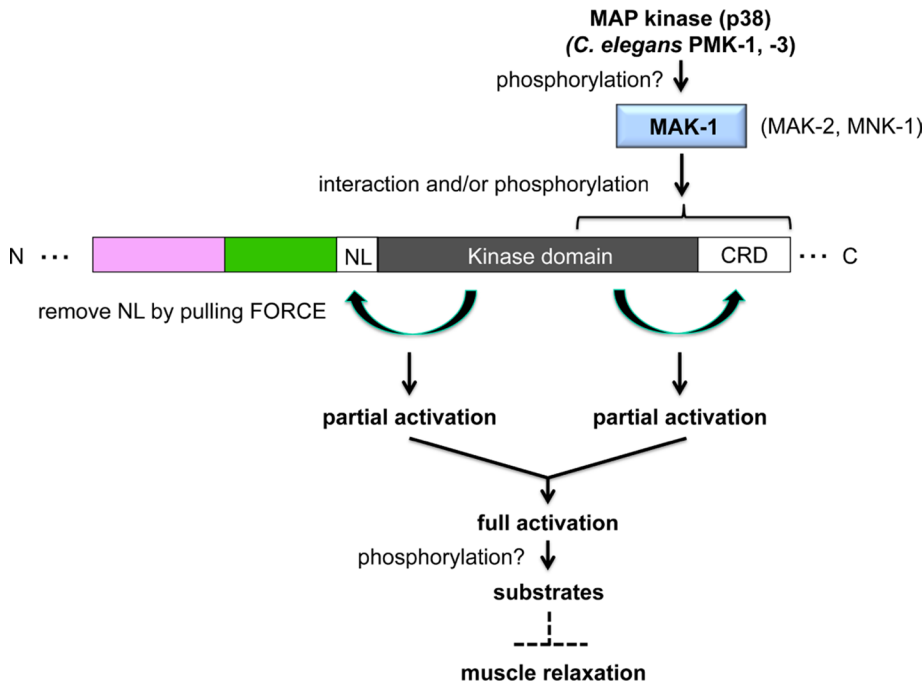


FIGURE 11: Speculative model for the function of MAK-1 in striated muscle cells. In vitro kinase assays of twitchin kinase show that NL and CRD each inhibits kinase activity by one-half. Molecular dynamic simulations indicate that the mechanically sensitive portion is NL, 45 residues lying between the Fn3 domain and the catalytic core, and that the CRD remains attached to the large lobe of the kinase even after the small lobe has been unwound (von Castellmur *et al.*, 2012). Therefore MAK-1 might contribute to the removal of the CRD segment from the catalytic core by binding or by phosphorylation. The nematode MAK-1 paralogues, MNK-1 and MAK-2, are also expressed in muscle, and each alone and the two in combination show partial resistance to nicotine. Thus MNK-1 and MAK-2, in addition to MAK-1, may be involved in activation. MAPKAP kinase 2 in mammals is activated by phosphorylation by p38 MAP kinase. The nematode orthologues of p38 MAP kinase include PMK-1 and -3. Their null mutants show an intermediate resistance to nicotine. Therefore it is possible that PMK-1 and -3 are also upstream components of this relaxation pathway. Rather than full activation, it is possible that partial activation by force and partial activation by MAK-1 occur independently to meet different physiological requirements.

His-tagged twitchin fragment (His-Kin, His-NL-Kin, His-Kin-CRD, His-NL-Kin-CRD) was resolved by SDS-PAGE and transferred to nitrocellulose membranes. The blots were incubated with 1 µg/ml MBP or MBP-MAK-1 (81–405), washed, and then reacted with anti-MBP conjugated to horseradish peroxidase (anti-MBP-horseradish peroxidase [HRP]; New England BioLabs, Ipswich, MA) at 1:5000 dilution and visualized by enhanced chemiluminescence (ECL; Pierce, Thermo Fisher Scientific, Waltham, MA). A pull-down assay was performed in the following manner: 5 µg of each His-tagged twitchin fragment (His-Kin, His-NL-Kin, His-Kin-CRD, His-NL-Kin-CRD) was separately incubated with 10 µg of either MBP or MBP-MAK-1 (81–405) in a total volume of 400 µl of binding/washing buffer (50 mM Tris, pH 7.5, 150 mM NaCl, 0.25% gelatin, 0.1% NP-40, and complete Mini protease inhibitors [Roche, Indianapolis, IN]) for 3 h at 4°C. Then to each reaction was added 50 µl of a 1:1 suspension of anti-His antibody-conjugated agarose beads (Medical and Biological Laboratories, Nagoya, Japan) with incubation with shaking for 1 h at 4°C. After four washes with binding/washing buffer, proteins were eluted from the beads with 30 µl of Laemmli buffer and heating at 95°C for 5 min. The eluted proteins were separated by SDS-PAGE and transferred to a blot; the transferred proteins were visualized by Ponceau S staining (Figure 3B, bottom), reacted with anti-MBP-HRP, and detected by ECL.

Transgenic animals for determining tissue expression of *mak-1*, *mak-2*, and *mnk-1*

The following plasmids were constructed: *mak-1p::gfp* has a 6.4-kb genomic fragment that includes the putative promoter sequence upstream of *mak-1*, a putative 5'-untranslated region, initiator ATG, and the first 12 nucleotides of the coding sequence of *mak-1*, amplified by PCR with primers YHM22 and YHM23 and cloned into the pPD95.75 vector (kindly provided by Andrew Fire, Stanford University, Stanford, CA) using *Pst*I and *Bam*HI sites. *mak-2p::gfp* has a 3.0-kb genomic fragment that includes the putative promoter sequence upstream of *mak-2*, 5'-untranslated region, initiator ATG, and the first 24 nucleotides of the coding region of *mak-2*, amplified by PCR with primers YHM24 and YHM25 and cloned into pPD95.75 vector using *Sph*I and *Bam*HI sites. *mnk-1p (a)::gfp* has a 3.7-kb genomic fragment that includes the putative promoter sequence upstream of *mnk-1a*, 5'-untranslated region, initiator ATG, and the first 12 nucleotides of the coding region of *mnk-1a*, amplified by PCR with primers YHM26 and YHM27 and cloned into pPD95.75 vector using *Sph*I and *Sal*I sites. *mnk-1p (b)::gfp* has a 4.8-kb genomic fragment that includes putative promoter sequence upstream of *mnk-1b*, 5'-untranslated region, initiator ATG, and the first 12 nucleotides of the coding region of *mnk-1b*, amplified by PCR with primers YHM28–YHM29 and cloned into pPD95.75 vector using *Sph*I and *Bam*HI sites. The constructed plasmids were injected at 20 ng/µl into the gonads of wild-type animals along with the pRF4 [*rol-6(su1006)*] plasmid as coinjection marker (80 ng/µl; Mello and Fire, 1995). At least three independent stable transgenic lines were generated for each plasmid.

Nematode strains

N2 (Bristol) is the primary wild-type strain, and standard growth conditions were used (Brenner, 1974). The following alleles were used in this study: *lev-1(e211)IV*, *mak-1(ok2987)II*, *mak-1(tm3455)II*, *mak-2(gk1110)IV*, *mnk-1(tm4266)III*, *pmk-1(km25)IV*, *pmk-3(ok169)IV*, *unc-22(e66)IV*, *unc-22(e105)IV*, *unc-22(ct37)IV*, *unc-29(e1072)I*, and *unc-63(x37)I*. The double-mutant animals *mak-1(ok2987); mak-2(gk1110)* and *mak-1(ok2987); mnk-1(tm4266)* were generated by crossing the respective single-mutant animals. To check for deletions of mutant animals, we carried out PCR with primers YHM31–YHM47. *mak-1(ok2987)* and *mak-1(tm3455)* were each outcrossed three times to wild type.

Mutation site in *mak-1(tm3455)*

Genomic DNA of the *mak-1* locus was amplified from *mak-1(tm3455)* mutant worms using nested PCR with designed primers (YHM48–YHM51). The deletion junction was determined by DNA sequencing.

Generation of antibodies to MAK-1 and immunoblot analysis

Residues 81–142 and 416–468 of MAK-1 were expressed and purified in *Escherichia coli* as glutathione S-transferase (GST) and MBP fusion proteins, respectively. To do this, each cDNA fragment was amplified by PCR (primers for aa 81–142: YHM5 and YHM52; primers for aa 416–468: YHM53 and YHM54) from *mak-1* cDNA clone (MAK-1 aa 81–521 fragment). cDNA fragments were cloned into pGEX-KK1 and pMAL-KK1 using *Bam*HI and *Xho*I sites. After finding an error-free clone, we expressed GST-fusion proteins as described in Mercer *et al.* (2006). The resulting GST-MAK-1(81-142) and GST-MAK-1(416-468) were shipped to Spring Valley Laboratories (Woodbine, MD) for generation of rabbit polyclonal antibodies. Anti-MAK-1 (81–142) and anti-MAK-1 (416–468) antibodies were affinity purified using Affigel conjugated to MBP-MAK-1 (81–142) or MBP-MAK-1 (416–468), as described previously (Mercer *et al.*, 2003).

Immunofluorescence localization

Adult nematodes were fixed using the method described previously (Nonet *et al.*, 1993; Wilson *et al.*, 2012). Primary antibodies were used at the following dilutions: anti-ATN-1 (α -actinin; MH35; Francis and Waterston, 1991) at 1:200, anti-MAK-1 (416–468) at 1:100, anti-myosin heavy chain A (MHC A; 5–6; Miller *et al.*, 1983) at 1:200, anti-myosin heavy chain B (MHC B; 5–8; Miller *et al.*, 1983) at 1:200, anti-PAT-6 (Warner *et al.*, 2013) at 1:200, anti-twitchin (I | II; Benian *et al.*, 1996) at 1:200, anti-UNC-52 (MH2; Rogalski *et al.*, 1993) at 1:200, anti-UNC-89 (MH42; Benian *et al.*, 1996) at 1:200, anti-UNC-95 at 1:200 (Qadota *et al.*, 2007), and anti-UNC-112 (Hikita *et al.*, 2005) at 1:200. For anti-MAK-1, anti-twitchin, anti-UNC-95, and anti-UNC-112, the secondary antibody was anti-rabbit Alexa 488 (Invitrogen). For anti-ATN-1, anti-MHC A, anti-MHC B, anti-UNC-52, and anti-UNC-89, the secondary antibody was anti-mouse Alexa 594 (Invitrogen, Grand Island, NY). For anti-PAT-6, the secondary antibody was anti-rat Alexa 594 (Invitrogen). Each secondary antibody was used at 1:200 dilution. Stained samples were mounted on a glass slide with a coverslip containing mounting solution (20 mM Tris, pH 8.0, 0.2 M Dabco, and 90% glycerol). Images were captured at room temperature with a Zeiss confocal system (LSM510) equipped with an Axiovert 100M microscope and an Apochromat 63 \times /1.4 numerical aperture oil objective in 2.5 \times zoom mode. The color balances of the images were adjusted by using Photoshop (Adobe, San Jose, CA).

Swimming assays

L4 animals of each genotype were picked to fresh OP50 plates and allowed to mature at 20°C for 24 h. The swimming assays were carried out on individual young adult animals in M9 buffer. For locomotion (swimming), body bends of individual young adult animals were counted for 1 min. A body bend was scored as a complete deflection of the anterior portion of the nematode from the midline. Approximately 20 animals of each genotype were analyzed.

Nicotine sensitivity assays using a WMicrotracker device

Synchronized young adult animals of each genotype were collected in M9 buffer. After a final wash with M9 buffer containing 0.01% Triton X-100 (M9T), a worm slurry (worm pellet:M9T = 1:5) was prepared. For the assays, 96-well plates were used. To each well was added 40 μ l of M9T followed by 10 μ l of slurry, delivering ~50–100 worms/well. The plate was placed in the dark at room temperature for 1 h. Then locomotive activities under no-nicotine conditions were measured for 1 h using a WMicrotracker (Phylumtech, Sante Fe, Argentina) with the program *C. elegans* (>L4) supplied by the

manufacturer. Supplemental Figure S2 shows the locomotive activities in 0% nicotine of all the worm strains used in these experiments. Supplemental Figure S2B also shows the behavior of several acetylcholine receptor mutants (*unc-29*, *unc-63*, and *lev-1*) in 0.05% nicotine as “positive controls,” since these are known to be resistant to nicotine (Gottschalk *et al.*, 2005). After the measurement, 50 μ l of M9T containing 0.2 or 0.1% nicotine solution was added to each well, and locomotive activities were measured using the WMicrotracker. For each strain and nicotine concentration, eight independent wells were assayed. On the graphs of locomotive activity versus time, each point represents the mean and SE. RNA interference (RNAi) of *unc-22* was performed by using an Ahringer library clone and the protocol described in Kamath *et al.* (2003).

Protein kinase assays with purified recombinant proteins

cDNA fragments containing the twitchin kinase domain (Fn31-Kinase-Ig26) harboring the K185A mutation, expected to abolish kinase activity, were amplified by PCR using primers *twcFnKinIlg-F*, *twcFnKinIlg-R*, YHM55, and YHM56 (see Supplemental Table S2). Derivatives of twitchin kinase fragments containing the K185A mutation were amplified by PCR using twitchin kinase with K-to-A cDNA as a template and the following primer combinations: *Twik-1* and *Twik-2* for NL-Kin-CRD, *Twik-3* and *Twik-2* for Kin-CRD, *Twik-1* and *Twik-4* for NL-Kin, and *Twik-3* and *Twik-4* for Kin only. *Bsm*BI-*Xho*I fragments of these twitchin kinase derivatives were cloned into the *Nco*I and *Xho*I sites of pETM11. To construct the His-tagged MAK-1 (aa 81–405) expression plasmid, cDNA was amplified by PCR using YHM57 and YHM4. The *Nco*I-*Xho*I fragment of this PCR product was cloned into *Nco*I/*Xho*I-cut pETM11. All of these plasmids were transformed into Rosetta 2 (DE3)-competent *E. coli* (EMD Millipore, Billerica, MA), and protein expression was induced with addition of 680 μ M isopropyl- β -D-thiogalactoside and grown for 5 h at 20°C for twitchin fragments and 15°C for MAK-1. Bacteria from a 500-ml culture were suspended in 30 ml of lysis buffer (50 mM Tris-HCl, 100 mM NaCl, 40 mM imidazole, 10 mM β -mercaptoethanol, 10% glycerol, pH 8.0, plus cOmplete Mini EDTA-free protease inhibitor cocktail [Roche]), and broken in a French pressure cell at 10,000 psi; after addition of 80 μ l of 20% Triton X-100 and 20 μ l of Benzonase nuclease (purity >90%; EMD Millipore) the lysate was centrifuged at 39,000 \times g for 45 min. To the cleared lysate was added 2 ml of a 50% suspension of Ni-agarose beads (Qiagen, Valencia, CA), which was mixed at 4°C for 30 min. The beads were pelleted and washed 5 \times in wash buffer (same as lysis buffer, but having 60 mM imidazole) and applied to a small column, and the protein was eluted with elution buffer (same as lysis buffer, but having 200 mM imidazole). Peak fractions were pooled and dialyzed against 50 mM Tris-HCl, pH 7.5, 150 mM NaCl, 5 mM MgCl₂, and 2 mM β -mercaptoethanol. Protein concentrations were determined by Bradford assays. Kinase assays were performed in the following manner. We first preincubated 1 μ g of each twitchin kinase fragment (K to A) with an equal molar amount of MAK-1 (81–405) in a volume of 15 μ l containing 50 mM Tris HCl, pH 7.5, 150 mM NaCl, 5 mM MgCl₂, and 0.05% Tween-20 at 25°C for 1 h with shaking. To this mixture was added 15 μ l of 50 mM Tris HCl, pH 7.5, 150 mM NaCl, 5 mM MgCl₂, 2 mM dithiothreitol, 0.05% Tween-20, 40 μ M ATP, and 1 μ Ci of [γ -³²P]ATP. After mixing, the solution was incubated at 30°C for 1 h, followed by addition of 7.5 μ l of 5 \times Laemmli sample buffer, heated at 95°C for 5 min, separated on a 10% polyacrylamide SDS gel, stained with Coomassie, destained, dried, and exposed to film overnight. SDS-PAGE showing the proteins used in this assay is shown in Figure 10C. For kinase assays in the reverse direction (twitchin kinase as enzyme, MAK-1 as substrate), the source of twitchin kinase was His-tagged twitchin kinase

domain only, which has been reported to be active (von Castelmur et al., 2012). As a substrate, full-length MAK-1 with the K-to-A mutation, also expected to abolish kinase activity, was amplified by PCR using YHM1, YHM2, YHM58, and YHM59 and cloned into pMAL-KK-1. MBP-MAK-1 (K to A) was purified as described previously (Mercer et al., 2006). The kinase assay was performed similarly to that described.

ACKNOWLEDGMENTS

We gratefully acknowledge grant support from the Human Frontier Science Program (RGP0044/2012) and the National Institutes of Health (AR064307). We thank Valery Baranets for help in determining the sequence of *unc-22(e105)*, Robert Barstead for the RB2 yeast two-hybrid library, Kozo Kaibuchi for vectors pGEX-KK and pMAL-KK, Andrew Fire for vectors for *C. elegans* promoter analysis, and Sergio Simonetta and Javier Bianchi at Phylumtech (Santa Fe, Argentina) for help in setting up the WMicrotracker. Some *C. elegans* strains were provided by the *Caenorhabditis* Genetics Center, which is funded by National Institutes of Health Office of Research Infrastructure Programs (P40 OD010440); other strains were obtained from the National Bioresource Project (Japan).

REFERENCES

Barstead RJ, Waterston RH (1989). The basal component of the nematode dense-body is vinculin. *J Biol Chem* 264, 10177–10185.

Benian GM, Kiff JE, Neckelmann N, Moerman DG, Waterston RH (1989). Sequence of an unusually large protein implicated in regulation of myosin activity in *C. elegans*. *Nature* 342, 45–50.

Benian GM, L'Hernault SW, Morris ME (1993). Additional sequence complexity in the muscle gene, *unc-22*, and its encoded protein, twitchin, of *Caenorhabditis elegans*. *Genetics* 134, 1097–1104.

Benian GM, Tinley TL, Tang X, Borodovsky M (1996). The *Caenorhabditis elegans* gene *unc-89*, required for muscle M-line assembly, encodes a giant modular protein composed of Ig and signal transduction domains. *J Cell Biol* 132, 835–848.

Ben-Levy R, Leighton IA, Doza YN, Attwood P, Morrice N, Marshall CJ, Cohen P (1995). Identification of novel phosphorylation sites required for activation of MAPKAP kinase-2. *EMBO J* 14, 5920–5930.

Berman K, McKay J, Avery L, Cobb M (2001). Isolation and characterization of *pmk-1-3*: three p38 homologs in *Caenorhabditis elegans*. *Mol Cell Biol Res Commun* 4, 337–344.

Bogomolovas J, Gasch A, Simkovic F, Rigden DJ, Labeit S, Mayans O (2014). Titin kinase is an inactive pseudokinase scaffold that supports MuRF1 recruitment to the sarcomeric M-line. *Open Biol* 4, 140041.

Brenner S (1974). The genetics of *Caenorhabditis elegans*. *Genetics* 77, 71–94.

Bullard B, Linke WA, Leonard K (2002). Varieties of elastic protein in invertebrate muscles. *J Muscle Res Cell Motil* 23, 435–447.

Butler TM, Siegman MJ (2011). A force-activated kinase in a catch smooth muscle. *J Muscle Res Cell Motil* 31, 349–358.

Ding L, Candido EPM (2000). HSP25, a small heat shock protein associated with dense bodies and M-lines of body wall muscle in *Caenorhabditis elegans*. *J Biol Chem* 275, 9510–9517.

Epstein HF, Thomson JN (1974). Temperature-sensitive mutation affecting myofilament assembly in *Caenorhabditis elegans*. *Nature* 250, 579–580.

Francis GR, Waterston RH (1991). Muscle cell attachment in *Caenorhabditis elegans*. *J Cell Biol* 114, 465–479.

Funabara D, Hamamoto C, Yamamoto K, Inoue A, Ueda M, Osawa R, Kanoh S, Hartshorne DJ, Suzuki S, Watabe S (2007). Unphosphorylated twitchin forms a complex with actin and myosin that may contribute to tension maintenance in catch. *J Exp Biol* 210, 4399–4410.

Gottschalk A, Almedom RB, Schedletsky T, Anderson SD, Yates JR III, Schafer WR (2005). Identification and characterization of novel nicotinic receptor-associated proteins in *Caenorhabditis elegans*. *EMBO J* 24, 2566–2578.

Grater F, Shen J, Jiang H, Gautel M, Grubmuller H (2005). Mechanically induced titin kinase activation studied by force-probe molecular dynamics simulations. *Biophys J* 88, 790–804.

Heierhorst J, Tang X, Lei J, Probst WC, Weiss KR, Kemp BE, Benian GM (1996). Substrate specificity and inhibitor sensitivity of Ca²⁺/S100-dependent twitchin kinases. *Eur J Biochem* 242, 454–459.

Hikita T, Qadota H, Tsuboi D, Taya S, Moerman DG, Kaibuchi K (2005). Identification of a novel Cdc42 GEF that is localized to the PAT-3-mediated adhesive structure. *Biochem Biophys Res Commun* 335, 139–145.

Hu SH, Parker MW, Lei JY, Wilce MC, Benian GM, Kemp BE (1994). Insights into autoregulation from the crystal structure of twitchin kinase. *Nature* 369, 581–584.

Iyer GH, Garrod S, Woods VL, Taylor SS (2005). Catalytic independent functions of a protein kinase as revealed by a kinase-dead mutant: study of the Lys72His mutant of cAMP-dependent kinase. *J Mol Biol* 351, 1110–1122.

Kamath RS, Ahringer J (2003). Genome-wide RNAi screening in *Caenorhabditis elegans*. *Methods* 30, 313–321.

Kemp BE, Pearson RB, Guerriero V, Bagchi IC, Means AR (1987). The calmodulin binding domain of chicken smooth muscle myosin light chain kinase contains a pseudosubstrate sequence. *J Biol Chem* 262, 2542–2548.

Kobe B, Heierhorst J, Feil SC, Parker MW, Benian GM, Weiss KR, Kemp BE (1996). Giant protein kinases: domain interactions and structural basis of autoregulation. *EMBO J* 15, 6810–6821.

Kontogianni-Konstantopoulos A, Ackermann MA, Bowman AL, Yap SV, Bloch RJ (2009). Muscle giants: molecular scaffolds in sarcomerogenesis. *Physiol Rev* 89, 1217–1267.

Krüger M, Linke WA (2011). The giant protein titin: a regulatory node that integrates myocyte signaling pathways. *J Biol Chem* 286, 9905–9912.

Lange S, Xiang F, Yakovenko A, Vihola A, Hackman P, Rostkova E, Kristensen J, Brandmeier B, Franzen G, Hedberg B, et al. (2005). The kinase domain of titin controls muscle gene expression and protein turnover. *Science* 308, 1599–1603.

Larsen JK, Yamboliev IA, Weber LA, Gerthoffer WT (1997). Phosphorylation of the 27-kDa heat shock protein via p38 MAP kinase and MAPKAP kinase in smooth muscle. *Am J Physiol* 273, L930–940.

Lei J, Tang X, Chambers TC, Pohl J, Benian GM (1994). Protein kinase domain of twitchin has protein kinase activity and an autoinhibitory region. *J Biol Chem* 269, 21078–21085.

Mackinnon AC, Qadota H, Norman KR, Moerman DG, Williams BD (2002). *C. elegans* PAT-4/ILK functions as an adaptor protein within integrin adhesion complexes. *Curr Biol* 12, 787–797.

Mayans O, van der Ven PF, Wilm M, Mues A, Young P, Furst DO, Wilmanns M, Gautel M (1998). Structural basis for activation of the titin kinase domain during myofibrillogenesis. *Nature* 395, 863–869.

Meissner B, Warner A, Wong K, Dube N, Lorch A, McKay SJ, Khattra J, Rogalski T, Somasiri A, Chaudhry I, et al. (2009). An integrated strategy to study muscle development and myofibril structure in *Caenorhabditis elegans*. *PLoS Genet* 5, e1000537.

Mello C, Fire A (1995). DNA transformation. *Methods Cell Biol* 48, 451–482.

Mercer KB, Flaherty DB, Miller RK, Qadota H, Tinley TL, Moerman DG, Benian GM (2003). *Caenorhabditis elegans* UNC-98, a C2H2 Zn finger protein, is a novel partner of UNC-97/PINCH in muscle adhesion complexes. *Mol Biol Cell* 14, 2492–2507.

Mercer KB, Miller RK, Tinley TL, Sheth S, Qadota H, Benian GM (2006). *Caenorhabditis elegans* UNC-96 is a new component of M-lines that interacts with UNC-98 and paramyosin and is required in adult muscle for assembly and/or maintenance of thick filaments. *Mol Biol Cell* 17, 3832–3847.

Miller DM, Ortiz I, Berliner GC, Epstein HF (1983). Differential localization of two myosins within nematode thick filaments. *Cell* 34, 477–490.

Miller RK, Qadota H, Landsverk ML, Mercer KB, Epstein HF, Benian GM (2006). UNC-98 links an integrin-associated complex to thick filaments in *Caenorhabditis elegans* muscle. *J Cell Biol* 175, 853–859.

Moerman DG, Baillie DL (1979). Genetic organization in *C. elegans*: fine-structure analysis of the *unc-22* gene. *Genetics* 91, 95–103.

Moerman DG, Benian GM, Barstead RJ, Schriefer LA, Waterston RH (1988). Identification and intracellular localization of the *unc-22* gene product of *Caenorhabditis elegans*. *Genes Dev* 2, 93–105.

Moerman DG, Benian GM, Waterston RH (1986). Molecular cloning of the muscle gene *unc-22* in *C. elegans* by Tc1 transposon tagging. *Proc Natl Acad Sci USA* 83, 2579–2583.

Moerman DG, Plurad S, Waterston RH, Baillie DL (1982). Mutations in the *unc-54* myosin heavy chain gene of *C. elegans* that alter contractility but not muscle structure. *Cell* 29, 773–781.

Nakano A, Baines CP, Kim SO, Pelech SL, Downey JM, Cohen MV, Critz SD (2000). Ischemic preconditioning activates MAPKAPK2 in the isolated rabbit heart: evidence for involvement of p38 MAPK. *Circ Res* 86, 144–151.

Nonet ML, Grundahl K, Meyer BJ, Rand JB (1993). Synaptic function is impaired but not eliminated in *C. elegans* mutants lacking synaptotagmin. *Cell* 73, 1291–1305.

- Probst WC, Cropper EC, Heierhorst J, Hooper SL, Jaffe H, Vilim F, Beushausen S, Kupfermann I, Weiss KR (1994). cAMP-dependent phosphorylation of *Aplysia* twitchin may mediate modulation of muscle contractions by neuropeptide cotransmitters. *Proc Natl Acad Sci USA* 91, 8487–8491.
- Puchner EM, Alexandrovich A, Kho AL, Hensen U, Schäfer LV, Brandmeier B, Gräter F, Grubmüller H, Gaub HE, Gautel M (2008). Mechanoenzymatics of titin kinase. *Proc Natl Acad Sci USA* 105, 13385–13390.
- Puchner EM, Gaub HE (2010). Exploring the conformation-regulated function of titin kinase by mechanical pump and probe experiments with single molecules. *Angew Chem Int Ed Engl* 49, 1147–1150.
- Qadota H, Anraku Y, Botstein D, Ohya Y (1994). Conditional lethality of a yeast strain expressing human RHOA in place of RHO1. *Proc Natl Acad Sci USA* 91, 9317–9321.
- Qadota H, McGaha LA, Mercer KB, Stark TJ, Ferrara TM, Benian GM (2008). A novel protein phosphatase is a binding partner for the protein kinase domains of UNC-89 (Obscurin) in *Caenorhabditis elegans*. *Mol Biol Cell* 19, 2424–2432.
- Qadota H, Mercer KB, Miller RK, Kaibuchi K, Benian GM (2007). Two LIM domain proteins and UNC-96 link UNC-97/pinch to myosin thick filaments in *Caenorhabditis elegans* muscle. *Mol Biol Cell* 18, 4317–4326.
- Rogalski TM, Williams BD, Mullen GP, Moerman DG (1993). Products of the *unc-52* gene in *Caenorhabditis elegans* are homologous to the core protein of the mammalian basement membrane heparan sulfate proteoglycan. *Genes Dev* 7, 1471–1484.
- Scharf M, Neef S, Freund R, Geers-Knorr C, Franz-Wachtel M, Brandis A, Krone D, Schneider H, Groos S, Menon MB, et al. (2013). Mitogen-activated protein kinase-activated protein kinases 2 and 3 regulate SERCA2a expression and fiber type composition to modulate skeletal muscle and cardiomyocyte function. *Mol Cell Biol* 33, 2586–2602.
- Seisenbacher G, Hafen E, Stocker H (2011). MK2-dependent p38b signaling protects *Drosophila* hindgut enterocytes against JNK-induced apoptosis under chronic stress. *PLoS Genet* 7, e1002168.
- Shiroto K, Otani H, Yamamoto F, Huang CK, Maulik N, Das DK (2005). MK2-/- gene knockout mouse hearts carry anti-apoptotic signal and are resistant to ischemia reperfusion injury. *J Mol Cell Cardiol* 38, 93–97.
- Siegmán MJ, Funabara D, Kinoshita S, Watabe S, Hartshorne DJ, Butler TM (1998). Phosphorylation of a twitchin-related protein controls catch and calcium sensitivity of force production in invertebrate smooth muscle. *Proc Natl Acad Sci USA* 95, 5383–5388.
- Stokoe D, Campbell DG, Nakielny S, Hidaka H, Leever SJ, Marshall C, Cohen P (1992a). MAPKAP kinase-2; a novel protein kinase activated by mitogen-activated protein kinase. *EMBO J* 11, 3985–3994.
- Stokoe D, Engel K, Campbell DG, Cohen P, Gaestel M (1992b). Identification of MAPKAP kinase 2 as a major enzyme responsible for the phosphorylation of the small mammalian heat shock proteins. *FEBS Lett* 313, 307–313.
- Stull JT, Nunnally MH, Michnoff CH (1986). Calmodulin-dependent protein kinases. In: *The Enzymes*, Vol. 17, ed. PD Boyer and EG Krebs, Orlando, FL: Academic Press, 113–166.
- Von Castelmur E, Strümpfer J, Franke B, Bogomolovas J, Barbieri S, Qadota H, Konarev PV, Svergun DI, Labeit S, Benian GM, et al. (2012). Identification of an N-terminal inhibitory extension as the primary mechanosensory regulator of twitchin kinase. *Proc Natl Acad Sci USA* 109, 13608–13613.
- Warner A, Xiong G, Qadota H, Rogalski T, Vogl AW, Moerman DG, Benian GM (2013). CPNA-1, a copine domain protein, is located at integrin adhesion sites, and is required for myofilament stability in *C. elegans*. *Mol Biol Cell* 24, 601–616.
- Waterston RH, Thomson JN, Brenner S (1980). Mutants with altered muscle structure of *Caenorhabditis elegans*. *Dev Biol* 77, 271–302.
- Wilson KJ, Qadota H, Benian GM (2012). Immunofluorescent localization of proteins in *Caenorhabditis elegans* muscle. *Methods Mol Biol* 798, 171–181.
- Zengel JM, Epstein HF (1980). Identification of genetic elements associated with muscle structure in *C. elegans*. *Cell Motil* 1, 73–97.
- Zu YL, Ai Y, Gilchrist A, Maulik N, Watras J, Sha'afi RI, Das DK, Huang CK (1997). High expression and activation of MAP kinase-activated protein kinase 2 in cardiac muscle cells. *J Mol Cell Cardiol* 29, 2159–2168.